Full Paper

Development of the Enabling Route for Glecaprevir via Ring Closing Metathesis

Russell D Cink, Kirill Lukin, Richard D Bishop, Gang Zhao, Matthew J Pelc, Timothy B Towne, Bradley D Gates, Matthew M Ravn, David R Hill, Chen Ding, Steven C. Cullen, Jianzhang Mei, M. Robert Leanna, Jeremy Henle, Jose G Napolitano, Nandkishor Nere, Shuang Chen, Ahmad Y. Sheikh, and Jeffrey M. Kallemeyn

Org. Process Res. Dev., **Just Accepted Manuscript** • DOI: 10.1021/acs.oprd.9b00469 • Publication Date (Web): 27 Dec 2019

Development of the Enabling Route for Glecaprevir via Ring Closing Metathesis

Russell D. Cink, Kirill A. Lukin, Richard D. Bishop, Gang Zhao, Matthew J. Pelc, Timothy B. Towne, Bradley D. Gates, Matthew M. Ravn, David R. Hill, Chen Ding,† Steven C. Cullen, Jianzhang Mei, M. Robert Leanna, Jeremy Henle, José G. Napolitano, Nandkishor K. Nere, Shuang Chen, Ahmad Sheikh, and Jeffrey M. Kallemeyn*

Process Research & Development, AbbVie Inc., 1401 Sheridan Road, North Chicago, IL, 60064

For Table of Contents Only (first is 1200 dpi, second is 300 dpi, third is chemdraw)

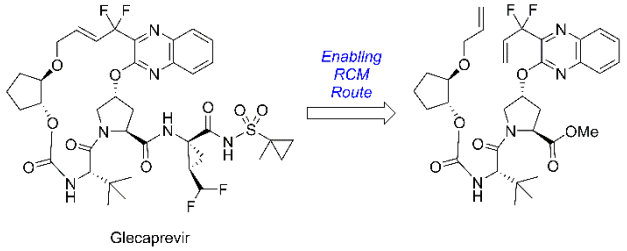

Glecaprevir

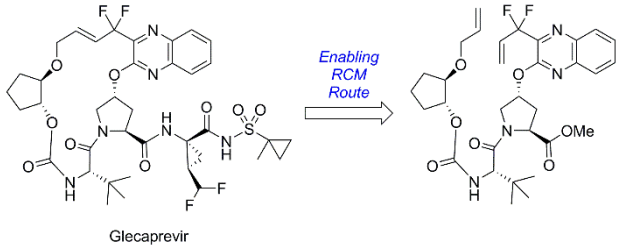

Glecaprevir

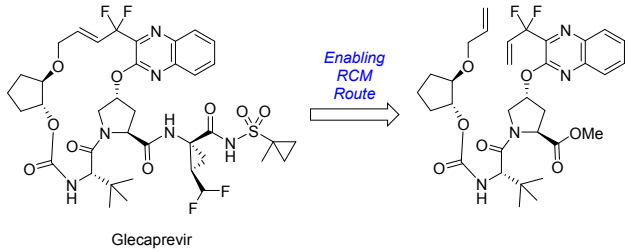

Glecaprevir

KEYWORDS

glecaprevir, ABT-493, ring closing metathesis, HCV

Abstract: Glecaprevir was identified as a potent HCV NS3/4A protease inhibitor and an enabling synthesis was required to support the pre-clinical evaluation and subsequent Phase I clinical trials. The enabling route to glecaprevir was established through further development of the medicinal chemistry route. The key steps in the synthesis involved a ring closing metathesis (RCM) reaction to form the 18-membered macrocycle, and a challenging fluorination step to form a key amino acid. The enabling route was successfully used to produce 41 kg of glecaprevir, sufficient to support the pre-clinical evaluation and early clinical development.

Introduction

The hepatitis C virus (HCV) is a blood borne disease estimated to affect between 71 and 185 million people throughout the world.[1] Persons infected with HCV can show no signs of the disease for decades. Left untreated HCV can lead to liver failure, liver cancer, and ultimately death. One of the challenges in developing treatments is the genetic heterogeneity of HCV, with six major genotypes identified. Fortunately, the development of combinations of direct acting antiviral agents in recent years has resulted in multiple treatment options that represent a curative therapy for all major HCV genotypes.[2]

In December 2006, Abbott Laboratories, which subsequently split to form AbbVie, began a collaborative effort with Enanta Pharmaceuticals focused on the development of HCV protease inhibitors. The collaboration led to the development of ABT-450 as part of AbbVie's first generation products for HCV treatment.[3] The first generation products were multi-drug combinations that were limited to the treatment of patients with genotypes 1a, 1b, and 4. A second generation program was initiated to discover and develop a treatment with broad genotypic activity that required fewer active ingredients in the combination. Glecaprevir was identified as a potent HCV NS3/4A protease inhibitor with pan-genotypic activity.[4] Glecaprevir

was developed in combination with pibrentasvir, an NS5A inhibitor which also exhibits pan-genotypic activity. The combination of glecaprevir and pibrentasvir was approved for the treatment of chronic hepatitis C virus genotypes 1–6.[5]

An enabling synthesis of glecaprevir was required to support the pre-clinical evaluation and subsequent Phase I clinical trials. The retrosynthetic analysis for the medicinal chemistry route to glecaprevir (**1**), as shown in Scheme 1, began with an initial disconnection of the amide bond dissecting glecaprevir (**1**) into amino sulfonamide **2** and macrocyclic acid **3**. The amino sulfonamide **2** was prepared from sulfonamide **7** and amino acid **8**. The key step in the synthesis of amino acid **8** was the fluorination of the precursor aldehyde **9**. The key step in the synthesis of macrocyclic acid **3** was a ring closing metathesis reaction (RCM) of diene **4**, which was in turn derived from coupling of carbamate **5** with amine **6**.[6]

Scheme 1. Retrosynthetic Analysis of the Enabling Route to Glecaprevir

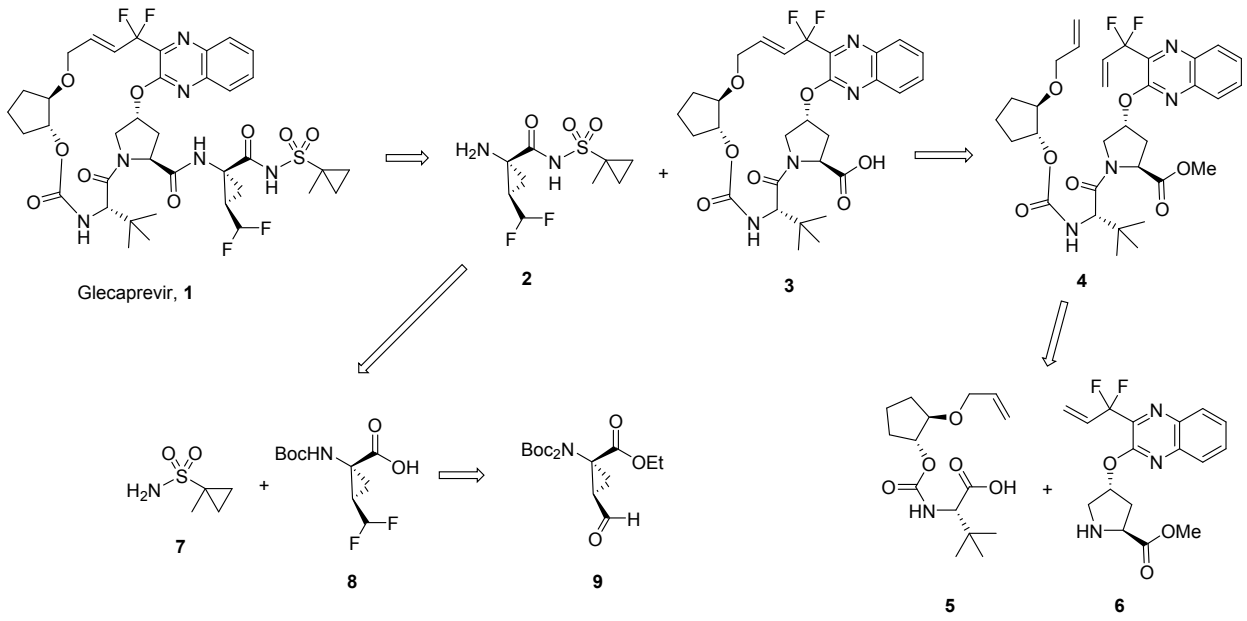

Given the structural complexity of glecaprevir (**1**) and the time constraints of the project, the strategy for the preparation of initial batches of glecaprevir (**1**) was to utilize the same major

disconnections as the existing medicinal chemistry route while implementing improvements to enhance the scalability of the synthesis. An evaluation of the medicinal chemistry route revealed two major challenges and two minor challenges for the large-scale synthesis of **1**.

The first major challenge was the fluorination of aldehyde **9** which proceeded in less than 50% yield, employed the hazardous reagent diethylaminosulfur trifluoride (DAST), and resulted in recovery of unreacted starting material upon chromatographic purification.[7] The first key objective was the development of a fluorination procedure suitable to meet the short-term material requirements of the program. Due to the hazardous nature of DAST and similar reagents, this fluorination step was recognized as a serious limitation for this synthesis of amino acid **8**.[8] The strategy was to utilize this route for the initial production of **8** while an improved synthesis was being developed for larger scale production. The development of the synthetic route used for large scale production will be detailed in a subsequent publication.[9]

The second major synthetic challenge was the RCM reaction used to form macrocyclic acid **3** which proceeded in 59% yield, employed 9 mol % of the Zhan 1B catalyst, and required chromatographic purification.[10] Based on prior experience with similar substrates, a challenging purification was expected due to the likely formation of dimeric impurities and the *cis* alkene isomer. Therefore, the second key objective was the development of a reliable procedure for the RCM reaction that minimized the formation of dimeric impurities and the *cis* alkene isomer.

The two minor challenges were the reported low overall yields for the synthesis of amine **6** (34%) and carbamate **5** (12%).[10] The third key objective was therefore to develop robust processes that increased the yield for both amine **6** and carbamate **5**. With these three objectives in mind, the development of the enabling route to glecaprevir (**1**) began.

Results and Discussion

Synthesis of the Amino Acid 8

As shown in Scheme 2, the synthesis of aldehyde **9** began with the Boc amino ester **10**, synthesized in 6 steps and 29% yield from glycine ethyl ester.[11] The Boc amino ester **10** was first protected with an additional Boc group and the alkene was then subjected to osmium tetroxide catalyzed cleavage with sodium periodate to furnish aldehyde **9** in 75% overall yield.

Scheme 2. Synthesis of Aldehyde **9**

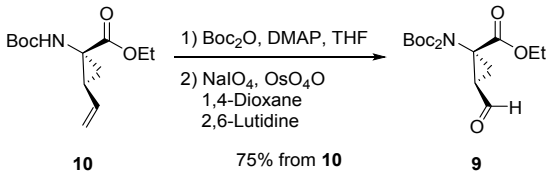

The subsequent fluorination reaction to form difluoro ester **11** proved to be particularly challenging. As shown in Table 1, the formation of a significant amount of side product **12** along with a small amount of alkene impurity **13** was observed. The formation of **13** is presumably the result of cyclopropane ring fragmentation of the initially formed mono-fluoro intermediate with concomitant addition of fluoride α to the ester. The formation of **12** is presumably the result of the ester carbonyl oxygen trapping the initially formed mono-fluoro intermediate, followed by fluoride addition to the ester carbonyl.[12] Side product **12** was stable under the reaction conditions but was not stable to reverse phase HPLC or silica gel chromatography due to hydrolysis back to the starting aldehyde **9**. The formation of side product **12** was the reason for recovery of unreacted starting material **9** upon chromatographic purification rather than incomplete conversion in the reaction. As a result, the reactions were best monitored by ^{1}H NMR to assess the conversion of aldehyde **9**, along with the amounts of **11**, **12** and **13** formed.[13] A parameter screen of the fluorination reaction was conducted in an effort to maximize the yield of **11** by minimizing the formation of side products **12** and **13**, and the results are summarized in Table 1.

Table 1. Screen of Fluorination Parameters for Aldehyde **9**

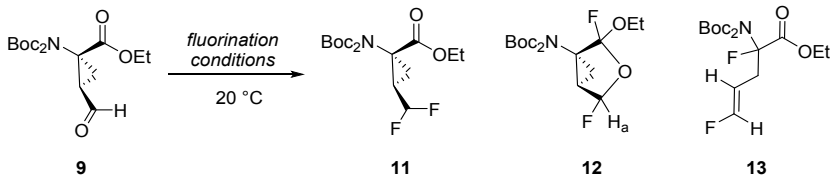

9 **11** **12** **13**

Entry	Reagent	Solvent	2,6-Lutidine	Ratio by ^{1}H NMR		
				11	**12**	**13**
1	Methyl DAST (4 equiv)	$CDCl_3$	0.25 equiv	50	46	4
2	Deoxo-Fluor® (4 equiv)	$CDCl_3$	none	45	52	3
3	Deoxo-Fluor® (2 equiv)	$CDCl_3$	0.25 equiv	31	69	0
4	DAST (4 equiv)	$CDCl_3$	none	50	41	9
5	DAST (4 equiv)	$CDCl_3$	0.1 equiv	51	45	4
6	DAST (4 equiv)	$CDCl_3$	0.2 equiv	50	47	3
7	DAST (4 equiv)	MeCN	none	15	56	29
8	DAST (4 equiv)	Toluene	none	50	46	4
9[a]	DAST (4 equiv)	Heptane	none	39	52	2
10[a]	DAST (4 equiv)	CH_2Cl_2	0.25 equiv	57	39	3
11	DAST (3.2 equiv)	CH_2Cl_2	0.2 equiv	55	41	4
12[a]	DAST (2.5 equiv)	CH_2Cl_2	0.25 equiv	53	40	4

(a) A small amount starting aldehyde **9** was present and accounts for the balance for these experiments.

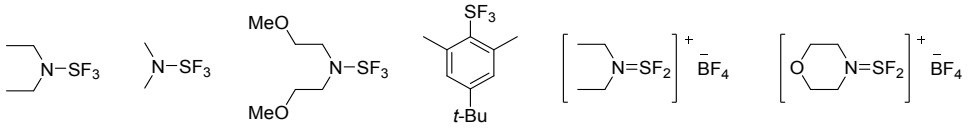

A screen of fluorination reagents was conducted and DAST, methyl DAST, and Deoxo-Fluor® gave the best conversion of aldehyde **9** to the difluoro ester **11**. Negligible conversion was observed with the alternative fluorination reagents Fluolead™, XtalFluor-E®, and XtalFluor-

M®.[14] DAST and Methyl DAST gave essentially the same profile (entries 1 and 6), whereas Deoxo-Fluor® showed less of product **11** and more of side product **12** (entries 2 and 3). The addition of a sub-stoichiometric amount of 2,6-lutidine was observed to reduce the level of alkene impurity **13** formed in the reaction for both DAST and Deoxo-Fluor® (entry 2 compared to 3, and entry 4 compared to 5 and 6). The addition of 2,6-lutidine also significantly slowed the reaction rate. Both observations are presumably due to the neutralization of HF in the reaction mixture. Other additives tested included EtOH, water, HF pyridine, BF_3 etherate, silica gel, and tetrabutylammonium difluorotriphenylsilicate (TBAT); all showed no improvement in the profile. Additionally, attempts to convert the side product **12** to the desired product **11** were unsuccessful when higher temperatures or more forcing conditions, including neat DAST, were employed. A solvent screen (entries 7 to 10) showed that toluene was comparable to $CDCl_3$, but CH_2Cl_2 produced the highest level of the desired product **11**. Evaluation of the reagent stoichiometry for the fluorination reaction (entries 10-12) showed the amount of DAST could be reduced to without impacting the product profile significantly. Based on these results, CH_2Cl_2 was selected as the reaction solvent and DAST (2.5 equiv) was selected as the fluorination reagent.

The primary challenge moving forward was the workup and in particular how to address the high level of the side product **12** formed in the reaction. It was found that upon hydrolysis of side product **12** back to starting material, the aldehyde **9** could be separated and recovered through conversion to the bisulfite adduct, as outlined in Scheme 3. For the process workup upon scale-up, the reaction mixture was quenched into aqueous K_2HPO_4 to consume the remaining DAST and extracted with heptane to give the crude product mixture containing **11**, **12** and **13**. The solution was then concentrated and mixed with aqueous KH_2PO_4 to hydrolyze side product **12**

back to the starting aldehyde **9**. The aldehyde **9** was then converted into the bisulfite adduct and separated into the aqueous layer while the product **11** and impurity **13** were extracted into heptane. The bisulfite adduct in the aqueous layer was then treated with sodium carbonate to regenerate the aldehyde **9** which crystallized from the mixture in 35% recovery relative to the starting amount of **9**. The average yield of **11** in the fluorination step was 40% over numerous batches. It was demonstrated that the recovered aldehyde **9** could be recycled through the fluorination step in the same yield.

Scheme 3. Synthesis of Amino Acid **8**

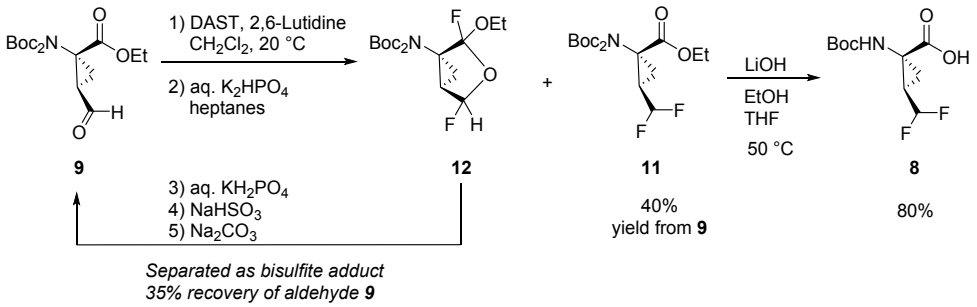

The difluoro ester **11** was then converted to the amino acid **8** in 80% yield. The use of LiOH was found to be important in cleanly removing the Boc group as NaOH resulted in a 2:1 mixture of mono-Boc and di-Boc acids at 20 °C with higher temperature resulting in lower yields. Impurity **13** underwent decomposition in the saponification and the resulting daughter impurities were rejected in the crystallization of amino acid **8**.

The yield of amino acid **8** was 24% from the Boc amino ester **10**, not accounting for a yield increase from recycle of recovered aldehyde **9** through the fluorination step. Although the process required a complicated workup sequence for the fluorination of aldehyde **9**, chromatography was eliminated from the process, with purification being accomplished by crystallization of aldehyde **9** and amino acid **8**. Taking into consideration the reported 29% yield

for the synthesis of Boc amino ester **10**, the overall yield of amino acid **8** was 7%.[11] The process outlined in Scheme 2 and Scheme 3 was conducted for the production of multiple batches amino acid **8**. This process met the objective of providing sufficient material for the early development of glecaprevir (**1**), but it was clear that this synthesis of amino acid **8** was not suitable for larger scale production. As mentioned earlier, the development of the synthetic route used for large scale production will be detailed in a subsequent publication.[9]

Synthesis of Amino Sulfonamide 2

With the synthesis of amino acid **8** in hand, the conversion to amino sulfonamide **2** was evaluated. As shown in Scheme 4, the coupling of amino acid **8** with the commercially available sulfonamide **7** was accomplished using HATU and DMAP. The coupling reaction required excess DMAP (4 equiv) to achieve good conversion and multiple aqueous washes to remove the DMAP. The Boc deprotection proceeded smoothly with HCl and the yield of amino sulfonamide **2** was 89% yield for the two-step sequence.

Scheme 4. Synthesis of Amino Sulfonamide **2**

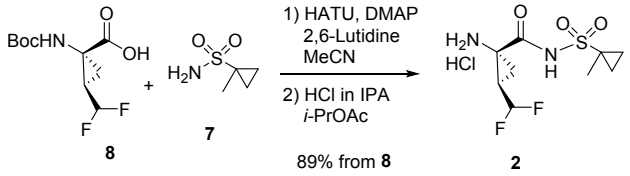

Synthesis of Carbamate 5

As shown in Scheme 1, the other main challenge was the synthesis of macrocyclic acid **3** which required the preparation of carbamate **5** and amine **6**. The retrosynthesis of carbamate **5**, as shown in Scheme 5, began with the dissection into *tert*-leucine **15** and the cyclopentane alcohol **14**, linked through the carbamate functionality. The coupling of the two fragments was planned through the use of a phosgene equivalent. The conversion of alcohol **14** into the

corresponding chloroformate was the preferred approach as this method had been successfully applied to the formation of carbamate linkages in structurally related targets. Conversion of *tert*-leucine **15** into the corresponding isocyanate was also considered, but typically requires the use of an excess of the alcohol (2 equiv) to achieve a good yield of the carbamate.[7] In this case the chiral alcohol **14** was the higher value material in the coupling, so it was preferable to use an excess of *tert*-leucine **15**. Based on prior experience with other related compounds, only a modest excess (1.2 equiv) of *tert*-leucine **15** would be required to form the carbamate bond.

Scheme 5. Retrosynthesis of Carbamate **5**

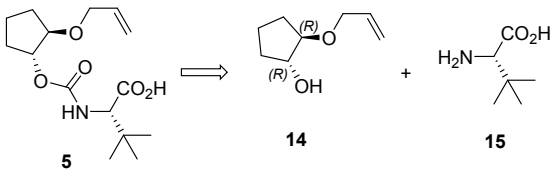

Evaluation of the medicinal chemistry route to intermediate **5** revealed some potential improvements to enhance the scalability of the synthesis. The chiral cyclopentane diol fragment was synthesized by an enzymatic resolution of the diacetate **16**, as shown in Scheme 6.[10] The resolution of diacetate **16** produced the desired mono-acetate **18** in 35% yield and was subsequently converted to the alcohol **14** in 40% yield. One of the known challenges with the resolution of diacetates such as **16** is that the product undergoes further conversion to the diol; in this case mono-acetate **18** is converted to the diol **19**.[15] This results in a lowering of the yield of **18**, and requires careful control of the reaction conditions to minimize over-reaction to form **19** as well as purification by chromatography.

Scheme 6. Initial Synthesis of Alcohol **14**

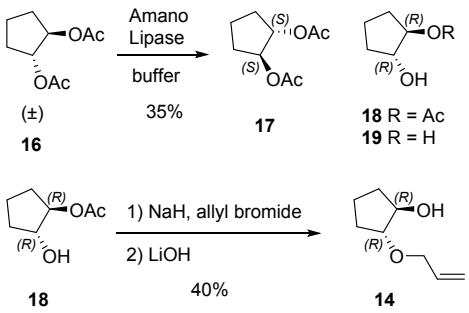

An alternate approach considered for the cyclopentane diol motif was to utilize a catalytic enantioselective epoxide opening of cyclopentene oxide, with three options outlined in Scheme 7. This approach has the advantage of potential higher yields as the *meso* epoxide can theoretically be quantitatively converted to a single stereoisomer. The cobalt salen catalyst developed by Jacobsen was known to produce the benzoate **20**, but in modest yield and chiral purity.[16] The oligomeric cobalt salen catalyst was reported to improve the yield and enantioselectivity for similar substrates, but was not commercially available.[17] The gallium BINOL catalysts developed by Shibasaki were known to produce the aryl ether **21** in good yield and chiral purity, but the high catalyst loading and additional deprotection steps were considered problematic for expeditious scale up of the process.[18] Zhao and co-workers reported an epoxide hydrolase (BD10721) was capable of producing diol **19** in good chiral purity, but this approach was not evaluated due to time constraints.[19]

Scheme 7. Alternate Syntheses of the Cyclopentyl Motif

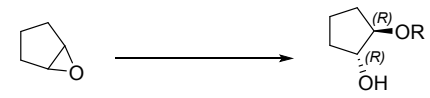

Option 1: Co Salen catalyst, BzOH **20:** R = Bz
Option 2: Ga BINOL catalyst, ArOH **21:** R = Ar
Option 3: Epoxide Hydrolase **19:** R = H

In order to simplify the resolution and separation of the enantiomers, an alternate sequence was developed as outlined in Scheme 8. The *trans* cyclopentane diol motif could be derived from cyclopentene oxide, and therefore the synthesis was modified to perform the ring opening of cyclopentene oxide with allyl alcohol to produce racemic, *trans* substituted alcohol **22**. Although some dimers and trimers were formed upon further reaction of alcohol **22** with cyclopentene oxide, the product was easily purified by distillation. Using this approach, the two alcohol functionalities of the cyclopentane were differentiated in preparation for an enzymatic resolution. After conversion to acetate **23**, the proposed enzymatic resolution (Table 2) would yield only two products, the undesired (*S*,*S*) acetate **24**, and the desired (*R*,*R*) alcohol **14**.[20]

Scheme 8. Synthesis of Acetate **23**

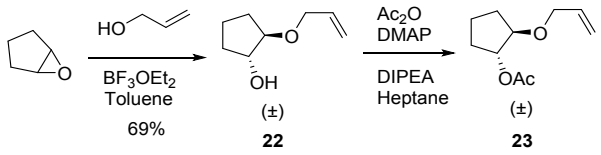

A screen of nineteen enzymes was conducted, and the results are summarized in Table 2 for the seven enzymes which showed conversion. The chiral purity of the product alcohol **14** was initially determined by derivatization as the Mosher ester and analysis by GC-MS, with the configuration determined by NMR analysis. The Codexis enzyme NZL-102-LYO, and the immobilized form NZL-102-IMB, showed excellent conversion and chiral purity (entries 2 and 5). The Fluka lipase from *Mucor miehei* (entry 7) also showed excellent chiral purity, but the reaction rate was significantly slower than entries 2 and 5. The enzyme in entries 2 and 5 was the same, simply either in lyophilized or immobilized form, and was *Candida Antarctica* Lipase B used to manufacture the commercially available immobilized enzyme Novozym 435.[21] As such, Novozym 435 was selected for further development of the resolution of **23**.

Table 2. Enzyme Screen for Resolution of Acetate **23**

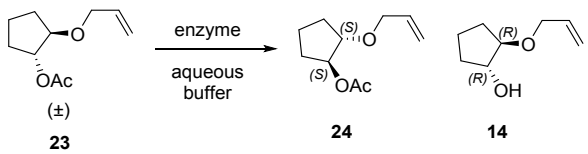

Entry	Enzyme[a]	ee	Config. **14**
1	Codexis NZL-101-LYO	0	
2	Codexis NZL-102-LYO	> 95%	(*R,R*)
3	Codexis NZL-107-LYO	0	
4	Codexis NZL-101-IMB	0	
5	Codexis NZL-102-IMB	> 95%	(*R,R*)
6	Sigma esterase E3019	0	
7	Fluka lipase from *Mucor miehei*	> 95%	(*R,R*)

(a) Reactions conducted using 0.25 mmol of **23** (neat) with 2.5 mL of 100 mM pH 7 phosphate buffer at 35 °C.

After development of a chiral HPLC method to allow more accurate characterization of the product, the resolution with Novozym 435 was found to be exceptionally robust, producing alcohol **14** in 47% overall yield from **22** with ≥ 99.8% ee (Scheme 9). It is noteworthy that the resolution showed no erosion of chiral purity of **14** even upon extended reaction times, indicating essentially no conversion of acetate **24**. As shown in Scheme 9, the mixture of acetate **24** and alcohol **14** was carried forward, with **14** being converted to the chloroformate **25** upon reaction with triphosgene. After an aqueous workup, the chloroformate **25** was isolated as a toluene solution that also contained the unreacted acetate **24**. The chloroformate **25** was coupled to *tert*-leucine **15** under biphasic conditions to produce carbamate **5** which was separated in the aqueous layer as the sodium carboxylate salt, with the unreacted acetate **24** being easily removed in the toluene layer. This simple strategy facilitated the separation of the enantiomers produced in the

enzymatic resolution without additional purification steps. The carbamate **5** was then isolated as the dicyclohexylamine ($NH(Cy)_2$) salt for purification.

Scheme 9. Conversion of Acetate **23** to Carbamate **5**

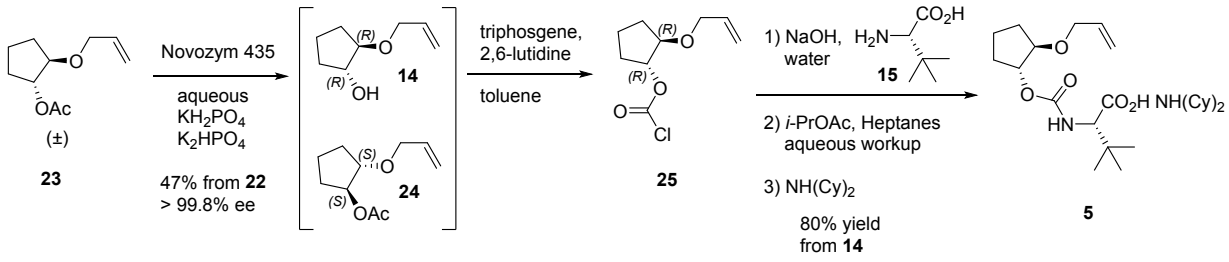

The overall 5 step sequence produced carbamate **5** in 26% yield from cyclopentene oxide, without chromatography and with only one distillation and one crystallization required for purification. By switching to a resolution of acetate **23** instead of resolution of diacetate **16**, the enabling process met the objective of increasing yield of carbamate **5** by more than doubling the 12% yield of the initial route.[10] Overall, the enabling process to carbamate **5** was simple, robust, and suitable for large scale production.

Synthesis of Amine 6

The strategy for the synthesis of amine **6**, as shown in Scheme 10, was to couple the commercially available hydroxyproline **26** with chloro quinoxaline **27** through a S_NAr reaction. This approach had been successful on several structurally related targets. The synthesis of chloro quinoxaline **27** was planned through condensation of diaminobenzene **29** with the keto ester **28** which contained the α-difluoro alkene functionality.

Scheme 10. Retrosynthesis of Amine **6**

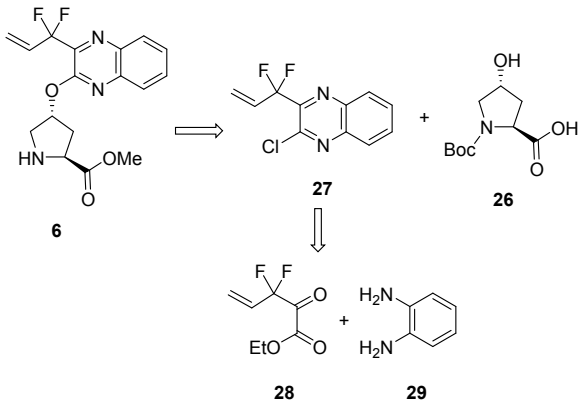

The synthesis of the amine **6**, shown in Scheme 11, began with the commercially available bromide **30** and ethyl glyoxylate **31**. Bromide **30** proved to be the most straightforward source of the required α-difluoro alkene functionality in keto ester **28**. Lithium halogen exchange of **30** had been reported but required cryogenic conditions, and the zinc species was shown to provide moderate yields upon addition to aldehydes and ketones.[22] The bromide **30** was known to form an allyl indium species suitable for alkylation of aldehydes.[23] The formation of the allyl indium species of **30** in a mixture of THF and water proved to be the ideal conditions for the addition to ethyl glyoxylate **31**.[24]

Scheme 11. Synthesis of Amine **6**

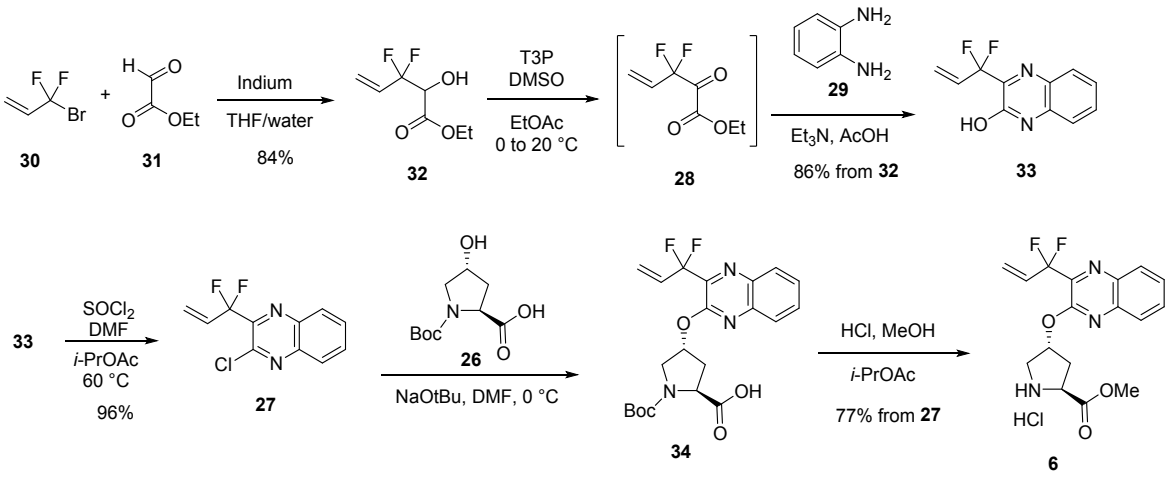

The formation of the allyl indium species was found to be sensitive to the mixing efficiency. In a lab scale cylindrical reactor with overhead stirring using a retreat curve agitator blade, the indium was observed to settle on the bottom of the reactor due to the high density of indium (7 g/mL), resulting in a 10% lower yield. In order to avoid this issue in larger scale batches, the reaction was run in a reactor with an agitator nearly touching the bottom of the reactor. Additionally, the reaction showed a 20% lower yield when exposed to air, so the reaction solvents were degassed to exclude oxygen from the reaction. With these modifications the yield of the alkylation of ethyl glyoxylate **31** was 84% based on the bromide **30** (93% based on **31**). A slight undercharge of ethyl glyoxylate (0.9 equiv) was used to minimize the formation of daughter impurities in the downstream process. The oxidation of **32** to the ketone **28** was initially conducted using either Dess-Martin periodinane or TPAP/NMO. Further evaluation revealed that the oxidation of **32** proceeded cleanly using T3P to activate DMSO at 0 °C.[25] In our hands, this reagent combination was found to be a generally mild oxidation reaction suitable for use with sensitive substrates and did not require added base to complete the oxidation. The switch to T3P/DMSO also avoided the need for controls for residual ruthenium with TPAP, and the safety

concerns associated with Dess-Martin periodinane. The ketone **28** was then condensed *in situ* with diaminobenzene **29** to give quinoxaline **33** which was isolated in 86% yield by crystallization from the reaction mixture. The enabling synthesis of quinoxaline **33** shown in Scheme 11 resulted in a 72% overall yield, and represents a significant increase compared to the 41% yield reported for the initial procedure.[10] The yield increase was the result of the improved conditions for the indium coupling to form alcohol **32** and implementing the T3P/DMSO oxidation to form ketone **28**.

The quinoxaline **33** was subsequently converted to the chloro quinoxaline **27**. Crystallization of **27** offered minimal purification so instead a silica plug filtration was used to remove color and polar impurities. The S_NAr reaction of chloro quinoxaline **27** with hydroxyproline **26** proceeded smoothly to form the acid **34** in nearly quantitative yield. The removal of the Boc protecting group and conversion to the methyl ester was accomplished using HCl in methanol, allowing for isolation of **6** as the hydrochloride salt from the reaction mixture after a solvent switch to isopropyl acetate. The crystallization of **6** was straightforward on lab scale but proved more challenging at large scale. The crystallization required removal of the excess HCl in order to achieve supersaturation, and this was accomplished by chase distillation with methanol. The efficiency of the HCl removal by chase distillation was reduced at large scale and required larger amounts of methanol. The starting 7.5 equivalents of HCl in the reaction were reduced to approximately 3 equivalents by chase distillation with methanol which induced crystallization. In the end the amine **6** was isolated in an average 77% yield from chloro quinoxaline **27**.

The amine **6** was produced in 53% overall yield from bromide **30**, with purification by crystallization at intermediates **33** and **6** and a silica plug filtration of intermediate **27**. The yield of amine **6** was increased by more than 50% compared to the 34% yield reported for the initial

procedure.[10] The enabling process met the objective of improving the yield for the synthesis of amine **6** due to the increased yields of the indium coupling to form **32** and the T3P/DMSO oxidation to form **28**.

Synthesis of the Macrocyclic Acid 3

With the efficient syntheses of **5** and **6** in hand, the preparation of macrocycle **35** could be achieved by an amide coupling followed by a ring closing metathesis (RCM) reaction, as shown in Scheme 12. The coupling of acid **5** with the amine **6** using HATU as the coupling reagent to produce diene **4** proceeded in quantitative yield; a significant increase compared to the initially reported 59%.[10] The diene **4** was purified by a silica plug filtration to ensure removal of potential catalyst poisons in preparation for the subsequent RCM reaction.

Scheme 12. Synthesis of the Macrocycle Ester **35**

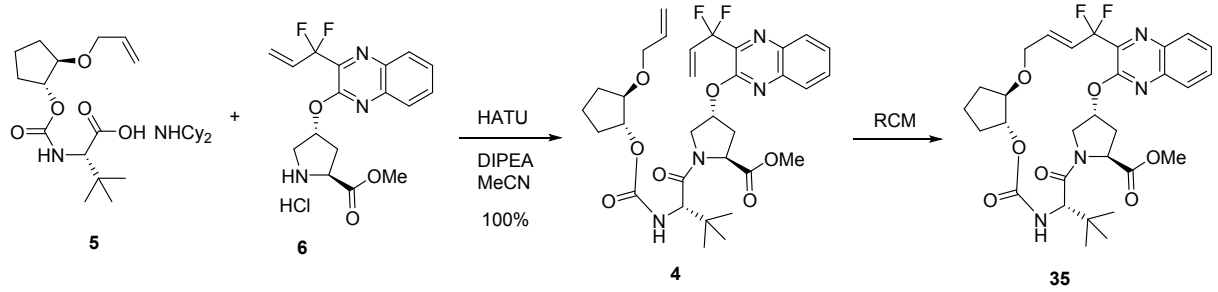

The RCM reaction proved to be a significantly challenging step in the synthesis. The reaction required a high catalyst loading in order to achieve near complete conversion and produced significant amounts of the *cis* isomer impurity **36** and the dimer impurity **37**, along with a low level of the Zhan 1B catalyst-derived impurity **38**. The structures of the RCM reaction impurities are shown in Figure 1.[26] It should be noted that the dimer impurity **37** was formed at higher levels early in the course of the reaction but gradually converted to product resulting in a lower final level.

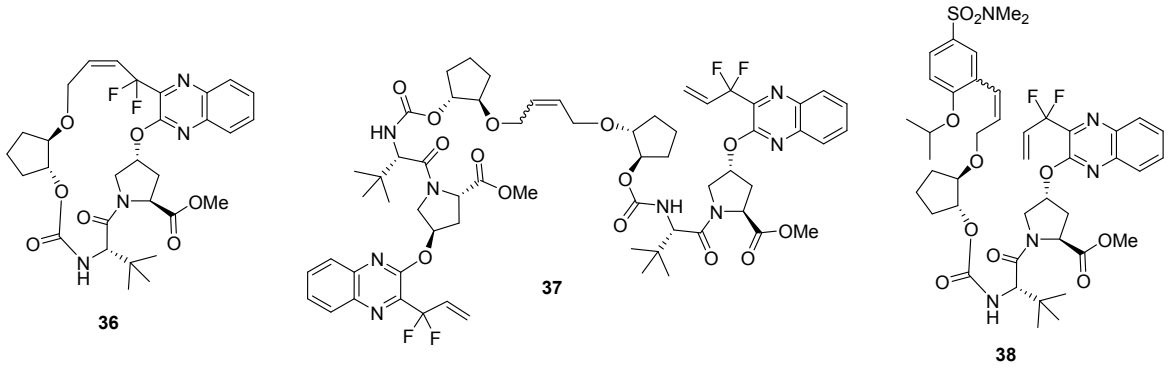

Figure 1. Impurities Formed in the RCM Reaction

A catalyst screen was conducted, shown in Table 3, and revealed that the Zhan 1B catalyst and the Grubbs second generation catalyst performed the best (entries 1 and 2), giving the highest conversion to **35** and similar levels of impurities **36** and **37**. The other catalysts screened (entries 4-8) showed either low yields of **35**, higher levels of the *cis* isomer impurity **36** relative to **35**, or high levels of dimer impurity **37**.[27] Based on literature precedent, the addition of acetic acid was also evaluated as a potential strategy to reduce the level of the *cis* isomer impurity **36** but this offered no improvement (entries 3, and 6, 7, and 8).[28] The Zhan 1B catalyst was selected for further evaluation as it provided the highest level of product and the lowest level of starting material.

Table 3. Catalyst Screen for the RCM Reaction

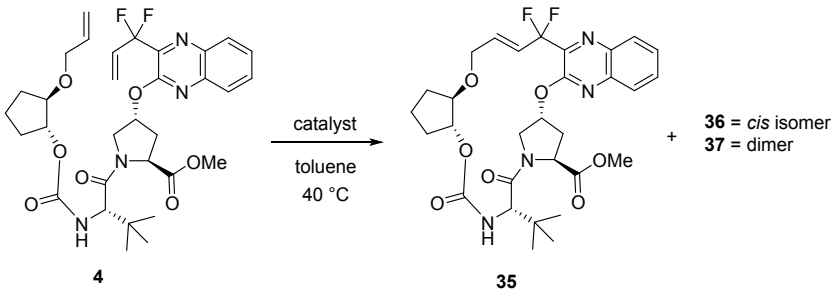

Entry	Catalyst[a]	Catalyst (mol %)	AcOH (equiv)	Ratio **35**/**36**	HPLC Area %			
					4	**35**	**36**	**37**
1	Zhan 1B	10	0	7.9	0.4	82	10.4	3.1
2	Grubbs 2nd Generation	10	0	7.5	4.6	79	10.5	3.1
3	Zhan 1B	5	0.5	7.6	6.2	75.2	9.9	8.7
4	Zhan 1B resin supported	3	0	-	~100	-	-	-
5	Grubbs C801	6	0	-	62.6	-	-	37.4
6	Omega CS1	5	0.5	5.8	24	43.4	7.5	25.1
7	CatMETium® RF1	4	0.8	7.1	53	25	3.5	7
8	Hoveyda-Grubbs 1st Generation	6	0.5	-	58.5	-	-	41.5

(a) Reactions conducted at 42 ± 7 mg of **4** in toluene (100 mL/g of **4**) at 40 °C.

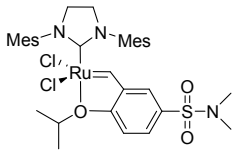
Zhan 1B

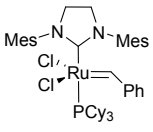
Grubbs 2nd Generation

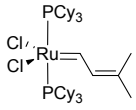
Grubbs C801

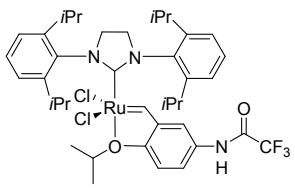
Omega CS1

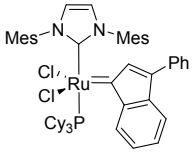
CatMETium® RF1

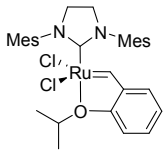
Hoveyda-Grubbs 1st Generation

A solvent screen showed the best impurity profile was obtained with toluene as compared to CH_2Cl_2, EtOAc, THF, and heptane/CH_2Cl_2. Through the screening experiments in Table 4 it was determined that lowering the reaction temperature reduced the amount of *cis* isomer impurity **36**

relative to the amount of product **35** (entries 1-4, ratio of **35**/**36**). However, at temperatures below 40 °C, the reactions were slower, required more catalyst, and showed higher levels of starting material **4** and the dimer impurity **37** (entries 3, 4). The reactions run below 40 °C frequently stalled and required multiple catalyst charges and extended reaction times to achieve reasonable conversion. As a result, the reaction temperature was set at 40 °C to minimize the *cis* isomer impurity **36** while allowing for near complete consumption of the starting material in a reasonable timeframe. At this temperature, the reaction was complete in approximately 20 h with 10% of the *cis* isomer **36** and 5% of the dimer impurity **37** (entry 7). A high catalyst loading of 8 mol % relative to **4** was required due to the reduced reactivity of the α-difluoro alkene in the substrate.[29] At lower catalyst loadings the reaction would stall out and require additional catalyst charges to restart the reaction, ultimately reaching 8 mol % of catalyst.

Table 4. Parameter Screen for the RCM Reaction

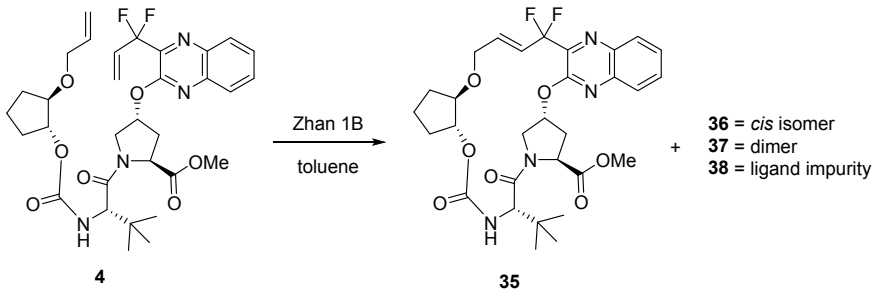

4 35

Entry	Temp (°C)	Toluene (mL/g **4**)	Reaction Time (h)	Addition Time (h)	Zhan 1B (mol %)	Ratio **35/36**	HPLC Area %				
							4	**35**	**36**	**37**	**38**
1 [b]	80	100	7[a]	4	8	4.8	1.5	74.9	15.5	6.1	1.5
2 [b]	40	100	24	6	10	8.3	2.2	81.7	9.8	5.1	0.8
3 [b]	30	100	100	7	13	9.0	8.5	73.5	8.2	6.4	1.9
4[c]	22	100	82	-	10	11.1	10.7	74.4	6.7	6.9	1.3
5[b]	40	20	45	6	8	9.4	1.2	78.0	8.3	7.6	3.2
6 [b]	40	40	50	6	8	8.6	1.5	78.7	9.2	7.9	2.2
7 [b]	40	80	26	6	8	8.4	0.6	82.0	9.8	5.3	0.8

(a) Mixed overnight at RT. (b) Reactions conducted using at least 1 g of **4**. (c) Reaction conducted using 95 mg of **4**.

The temperature dependence on formation of the *cis* impurity **36** was explored through a brief computational study. The ground state energies of the *cis* and *trans* macrocycle products were determined. The structures for **35** and **36** were optimized using DFT (B3 LYP-D3/6-31G*), and the solvated ground state energies with thermal corrections at 25/40/80 °C were calculated at the M06-2X/6-31G**/SM8(THF) level of theory (see the Supporting Information for details).[30] It was determined that at each temperature, the *cis* isomer had lower ground state energy by approximately 4.1 kcal/mol. This result, taken in conjunction with the observed *trans*/*cis* ratio dependence on temperature suggests the RCM reaction is operating under kinetic control; increasing the reaction temperature provides access to the pathway leading to the *cis* impurity. In

the optimized structures shown in Figure 2, the *trans* macrocycle has a "kink" in the backbone when compared to the *cis* isomer, especially noticeable in the positioning of the quinoxaline ring with respect to the backbone of the macrocycle. It is likely this feature that results in the increased ground-state energy of the *trans* macrocycle compared to the more open *cis* isomer.

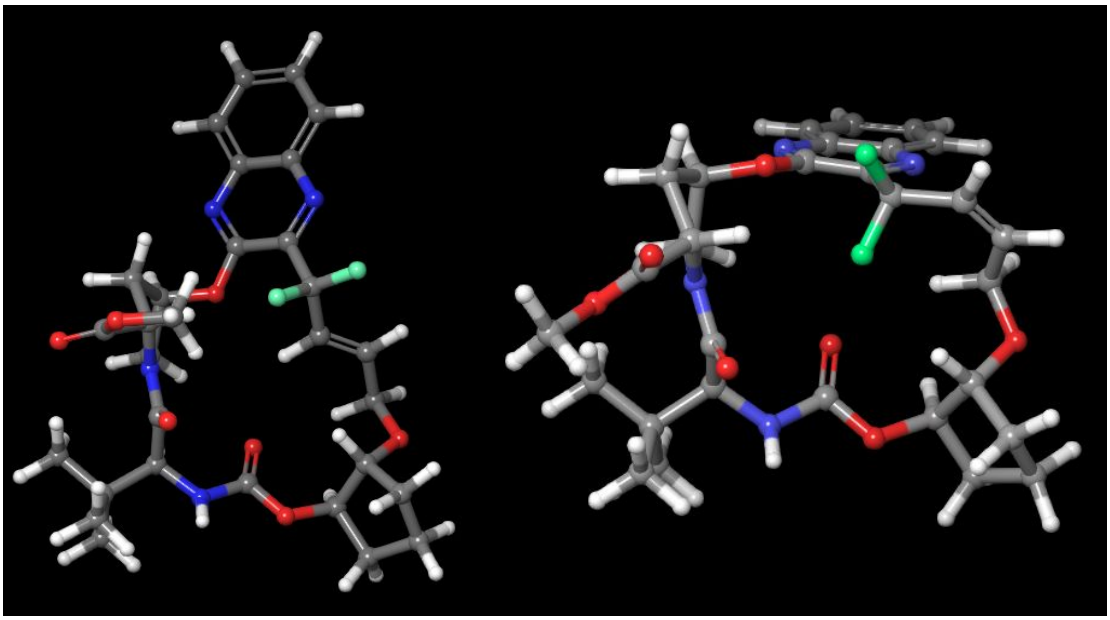

Figure 2. Left: DFT optimized structure of *trans* **35**. Right: DFT optimized structure of *cis* **36**.

A number of learnings from the RCM reaction in the ABT-450 process were implemented for this substrate, especially with regard to methods for minimizing formation of dimer impurities and driving the reaction to completion.[31] The reaction was conducted at high dilution (80 mL toluene per gram of **4**, 0.020 M) to minimize formation of the dimer impurity **37**. At higher concentrations, the reaction initially produced more dimer **37** which slowly converted to product **35**, but the final impurity profile was worse due to higher levels of the dimer impurity **37** and the ligand derived impurity **38** (Table 4, entries 5 and 6). With the exception of entry 4, the reactions in Table 4 were conducted with the simultaneous addition of separate solutions of catalyst and **4** over the same time period. The addition time of the solutions was approximately 6 hours but

ranged from 4 to 8 hours (Table 4). The slow addition of substrate to the large volume of toluene was intended to reduce the concentration of **4**, and therefore minimize dimer impurity **37** formation in favor of the desired product **35**. The slow addition of catalyst was intended to ensure active catalyst was present throughout the addition. The RCM reaction produced ethylene gas as a byproduct. Nitrogen sparging of the reaction mixture was used to remove the ethylene and drive the reaction to completion. A nitrogen sparge rate of 10-12 standard cubic feet per minute was implemented for scale up batches (Table 5).

With the preferred reaction conditions shown in entry 7 of Table 4, the product **35** also contained 10% of the *cis* isomer impurity **36**, 5% of the dimer impurity **37**, and 1-2% of both the starting material **4** and the ligand impurity **38**, along with 8 mol % of the catalyst. All of these contaminants had to be removed by the workup and purification or removed in the downstream processing. Crystallization of the macrocycle ester **35** was not effective for removal of the *cis* isomer impurity **36**, and instead crystallization of the next downstream intermediate, macrocyclic acid **3**, was determined to be the best point to reject the *cis* isomer impurity and other minor impurities. The dimer impurity **37** and its daughter impurities formed downstream in the synthesis of **3** and **1** were not effectively removed by crystallization. The method that completely removed the dimer impurity **37** with acceptable product loss was silica gel chromatography of intermediate **35**. The silica gel purification also removed the RCM catalyst and the ligand impurity **38**. After the reaction was complete, imidazole was added to quench the reaction. Filtrol was also added to the reaction mixture to adsorb the catalyst and improve the subsequent filtration rate. The first silica gel plug (2 g silica gel/g **4**) removed most of the catalyst, and the second silica gel plug (6-7 g silica gel/g **4**) removed the dimer impurity **37** and reduced the ruthenium level down to ~10 ppm. The amount of silica gel and the solvent gradient for the

second plug filtration were selected to minimize the amount required while ensuring complete removal of the dimer impurity **37**.

The first large scale RCM reactions (Table 5, runs 1 and 2) were conducted using 80 volumes of toluene at 40 °C, 8 mol % of catalyst, and a 6 hour addition of substrate and catalyst which consistently gave the best results in terms of yield, reaction time, and impurity profile. Further development for subsequent large scale batches showed that extending the addition time to 18 h allowed the reaction to be conducted at 40 volumes of toluene and produced a modest increase in yield while achieving a similar purity level post chromatography (Table 5, runs 3 and 4).

Table 5. Summary of Large-Scale RCM Reaction Results

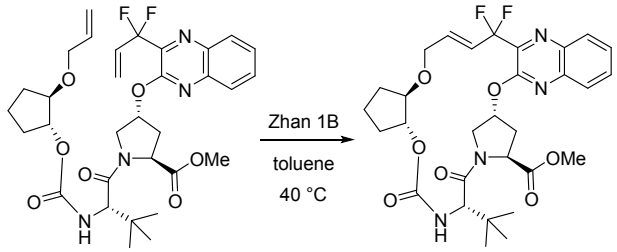

4 **35**

Parameters	Run 1	Run 2	Run 3	Run 4
Amount of **4** (kg)	19.7	19.7	20.0	20.0
Toluene (L/kg of **4**)	80	80	40	40
Addition Time (h)	6	6	18	18
Product **35** (area %)	87.2	86.0	88.7	88.1
Cis Isomer **36** (area %)	10.5	10.4	10.6	10.8
Starting Material **4** (area %)	2.3	3.6	0.5	1.0
Assay yield %	70.7	64.8	71.2	75.9

The conversion of the macrocycle ester **35** to the macrocyclic acid **3**, shown in Table 6, was straightforward and proved to be the best point in the process for rejection of the *cis* isomer impurity **39**. The reaction produced the expected 10% of the *cis* isomer impurity **39**, and after 4 crystallizations from 2-MeTHF and heptanes, the level of **39** was reduced to 1%. Although the solvent usage for four crystallizations was higher than desired, the process was simple, and the losses were modest as shown in Table 6. The overall yield for the conversion of the assayed amount the macrocycle ester **35** to the macrocyclic acid **3** was 84% which was remarkable given the degree of purification achieved.

Table 6. Saponification with Rejection of *cis* Isomer **39**

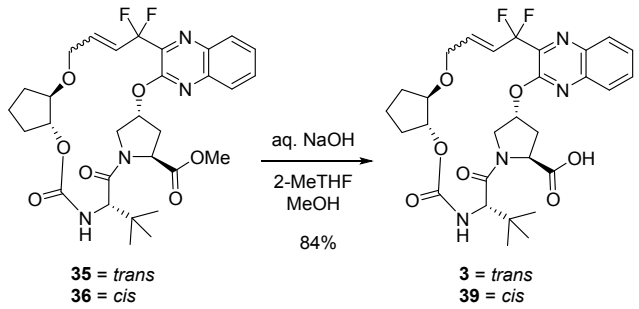

35 = *trans*
36 = *cis*

3 = *trans*
39 = *cis*

Sample	**3** (area %)	**39** (area %)	Loss of **3** (%)
Post Workup	85.4	10.5	0.8
1st Crystallization	93.4	6.1	2.5
2nd Crystallization	96.6	3.4	1.3
3rd Crystallization	97.9	2.1	1.3
4th Crystallization	99.0	1.0	1.5

The synthesis of macrocyclic acid **3** required three chromatographic purification steps and four crystallizations for a three-step yield of 57%. A more than 50% increase in yield for the enabling

process was achieved compared to the 35% yield reported for the same sequence in the initial process.[10] While the yield for the three step sequence to the macrocyclic acid **3** was acceptable and the process could be used to generate multi-kilogram batches, the process would be challenging for large scale production. The high RCM catalyst load and the reliance on silica gel chromatography would be prohibitive from a cost and throughput perspective. Additionally, the numerous crystallizations required to reduce the level of the *cis* isomer impurity **39** were also prohibitive. It was clear that although the RCM route was capable of producing macrocyclic acid **3**, a more efficient route to the macrocycle would be required for large scale production.[9]

Final Assembly of Glecaprevir

The final coupling of amino sulfonamide **2** with macrocyclic acid **3** was accomplished using EDAC and HOPO as the coupling reagents, as shown in Scheme 13. The coupling proceeded cleanly without detectable epimerization of the proline carboxylate. The reaction was initially run in dichloromethane with an aqueous workup to remove the reagent byproducts. The workup was laborious and offered negligible impurity removal. The reaction was found to proceed equally well in acetonitrile. The reaction was conducted in two reactors wherein the HOPO active ester of macrocyclic acid **3** was prepared in one reactor and then slowly added to the other reactor containing a mixture of amino sulfonamide **2** and triethylamine. Nearly complete conversion of macrocyclic acid **3** was achieved using this order of addition with only 1.1 equivalents of amino sulfonamide **2**.

Scheme 13. Final Coupling to Form Glecaprevir

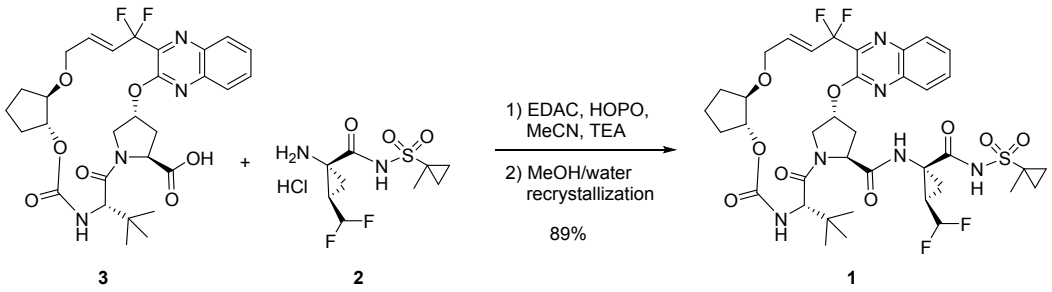

The switch to acetonitrile as the reaction solvent also offered the opportunity for direct crystallization after reaction completion. Upon quenching with aqueous acetic acid, the crude glecaprevir (**1**) crystallized from the reaction mixture. The addition of acetic acid was necessary to ensure protonation of the sulfonamide nitrogen and facilitate complete desupersaturation. The crystallization of the crude API was accomplished in 93% yield with rejection of the *cis* isomer daughter impurity to 0.37% from a starting level of 1.0% in macrocyclic acid **3**. The crude API was then recrystallized from methanol and water to obtain the mixed methanol-water solvate, which then was dried under vacuum to remove methanol followed by humidification to yield the desired hydrate crystal form.[32] The overall yield through the two crystallizations was 89%, with further rejection of the *cis* isomer daughter impurity to 0.15%. The process was used to prepare nine batches of glecaprevir (**1**) totaling 41 kg.

Conclusion

An enabling synthesis of glecaprevir (**1**) was developed to support the pre-clinical evaluation and subsequent Phase I clinical trials. The enabling route to glecaprevir (**1**) was established through further development of the medicinal chemistry route. The development of the fluorination of aldehyde **9** resulted in a reliable process suitable to meet the short term material requirements of the program, along with a better understanding of impurities generated in the

fluorination reaction. The workup for the fluorination reaction also allowed for recovery and recycle of the starting aldehyde **9** without the need for chromatography. The yield for the synthesis of carbamate **5** was more than doubled by switching to an enzymatic resolution of acetate **23**. The yield for the synthesis of amine **6** was increased by more than 50% by improvement of the indium coupling to form alcohol **23** and implementing the T3P/DMSO oxidation to form ketone **24**. The development of the macrocycle formation through the coupling to form diene **4** and the subsequent RCM reaction resulted in a more than 50% yield increase compared to the initial reported yield. Lowering the temperature of the RCM reaction resulted in less *cis* isomer impurity **36** and extending the addition time of the diene **4** resulted in less dimer impurity **37**. Implementing these process improvements, the enabling route was successfully used to produce 41 kg of glecaprevir (**1**) with an overall yield of 5.5% for the lowest yielding sequence in the synthesis of amino acid **8**.

Although the enabling route was acceptable to support the early development activities, an improved synthetic route would be required for large scale manufacturing. The key objectives for the development of the large scale synthetic route to glecaprevir (**1**) were improved syntheses for both macrocyclic acid **3** and amino acid **8**.[9] The creation of a new synthesis of macrocyclic acid **3** would require the development of a new method to form the 18-membered macrocycle. The creation of a new synthesis of amino acid **8** would require construction of the highly functionalized cyclopropane with control of stereochemistry. The syntheses for both macrocyclic acid **3** and amino acid **8** would also require installation of the difluoro functionality within both targets.

Experimental Section

General Information: All reagents and solvents were purchased from commercial vendors and used without further purification. Filtrol F1 grade was manufactured by BASF. ^{1}H NMR spectra were recorded on either a 400 or 600 MHz spectrometer, and chemical shifts (δ) are referenced to either TMS or the NMR solvent. ^{13}C NMR spectra were obtained at 101 or 151 MHz and referenced to the NMR solvent. ^{19}F NMR spectra were obtained at 564 MHz and referenced to C_6F_6.

HPLC samples were analyzed using an Agilent 1200 system equipped with a UV-DAD detector. Numerous HPLC methods were developed for the analysis of the reactions and products. The HPLC columns were typically an Ascentis Express C8 or C18 column (or equivalent), 10 or 15 cm × 4.6 mm, and 2.7 micron. The mobile phases were acetonitrile and either 0.1% H_3PO_4 or 0.1% $HClO_4$ with a gradient from 10% acetonitrile to 90% acetonitrile over 10 to 15 minutes. LC-MS samples were analyzed using similar methods with the exceptions of using 0.1% formic acid in both the aqueous and the acetonitrile mobile phases, and an ESI detector in positive ion mode.

Analysis by GC was conducted on an Agilent J&W HP-5 column, 30 m × 0.32 mm ID × 0.2 μm film thickness. For method A the injection temperature was 150 °C, the initial column temperature was 50 °C with a 10 °C/min ramp rate to 200 °C and a 10 min hold at 200 °C. The retention times of the compounds analyzed using method A are: allyl alcohol at 4.0 min, cyclopentene oxide at 5.2 min, alcohols **14** and **22** at 10.8 min, acetates **23** and **24** at 12.7 min, and chloroformate **25** at 13.3 min. For method B the injection temperature was 130 °C, the initial column temperature was 30 °C with a 10 °C/min ramp rate to 180 °C and a 10 min hold at 180 °C. The retention times of the compounds analyzed using method B are: bromide **30** at 4.0 min, ethyl glyoxylate **31** at 5.7 min, alcohol **32** at 10.4 min, and ketone **28** at 8.7 min.

The chiral purity of alcohol **14** was determined by HPLC using UV detection at 205 nm and two columns connected in series, a CHIRALPAK AS-3R, 150 × 4.6 mm, 3 μm and a CHIRALPAK AS-RH, 150 × 4.6 mm, 5 μm. The mobile phases were water and acetonitrile with an isocratic hold at 30% acetonitrile for 12 min, followed by a gradient to 90% acetonitrile. The desired (*R*,*R*) alcohol **14** eluted at 11.7 min and the (*S*,*S*) enantiomer at 10.8 min.

Aldehyde 9: Into a round bottom flask was charged **10** (11.2 g, 43.9 mmol) dissolved in THF (16 mL). To this solution was charged DMAP (5.62 g, 46.1 mmol, 1.05 equiv). To the resulting slurry was added a solution of $(Boc)_2O$ (14.36 g, 66.0 mmol, 1.5 equiv) in THF (10 mL) via a syringe, over 45 minutes at room temperature. The reaction mixture was quenched after 4.5 hours by addition of *N*,*N*-dimethylethylenediamine (3.87 g, 44 mmol, 1.0 equiv) in one portion. The quenched reaction was mixed 30 minutes, then poured into heptanes (50 g) and 1 M H_3PO_4 (120 g). The layers were separated and the upper layer was washed with 23% brine (50 mL). The upper product-containing layer was concentrated in vacuo to afford 16.98 g of a light orange oil. The oil was dissolved in 1,4-dioxane (70 mL) and 2,6-lutidine (7.25 g, 67.8 mmol, 1.5 equiv) and was then slowly charged over 4 hours into a flask containing $NaIO_4$ (42.28 g, 198.0 mmol, 4.5 equiv), water (90 g), 2,6-lutidine (2.14 g, 20 mmol, 0.45 equiv) OsO_4 (5.57 mL of a 4 wt% solution in water (0.88 mmol, 0.02 equiv)) and 1,4-dioxane (200 mL). The internal temperature was maintained below 30 °C during the addition. Additional $NaIO_4$ (4.7 g, 22.0 mmol, 0.5 equiv) was charged in one portion to the reaction mixture (slurry). The reaction mixture was cooled and a solution of 10% sodium thiosulfate (125 mL) was charged over 15 minutes. The precipitated $NaIO_3$ was filtered off and was washed with 1,4-dioxane (3 × 25 mL). The filtrate was extracted with heptane (200 mL). The layers were separated, and the aqueous layer was re-extracted with a 4:1 Heptane-MTBE solution (200 mL). The combined organic layers were washed sequentially

with 7% $NaHCO_3$ solution (100 mL), 1 M H_3PO_4 (100 mL), an solution comprised of 20 mL of 10% NaH_2PO_4 solution and 80 mL of 20% brine, 7% $NaHCO_3$ solution (100 mL) and finally washed with 20% brine (50 mL). The organic layer was then concentrated in vacuo and chased with heptane (40 g), concentrating in vacuo to 15.8 g. The product was crystallized from heptane (16 g) at -25 °C, filtered and washed twice with 5 mL of -20 °C heptane, and dried to constant weight to afford aldehyde **9** (11.78 g) in 75% yield. Aldehyde **9** can alternatively be crystallized from *i*-PrOH/water with cooling to 0 °C for filtration. ^{1}H NMR (400 MHz, $CDCl_3$) δ 9.46 (d, J = 5.7 Hz, 1H), 4.23 (qd, J = 7.1, 1.7 Hz, 2H), 2.48 (dd, J = 8.5, 6.3 Hz, 1H), 2.29 (ddd, J = 9.6, 8.5, 5.7 Hz, 1H), 1.78 (dd, J = 9.6, 6.3 Hz, 1H), 1.49 (s, 18H), 1.27 (t, J = 7.1 Hz, 3H). ^{13}C NMR (101 MHz, $CDCl_3$) δ 196.74, 169.10, 151.00, 83.62, 62.46, 46.18, 42.33, 28.38, 24.70, 14.67. HRMS calcd $C_{17}H_{27}NNaO_7$ $[M+Na]^+$: 380.1680, Found 380.1697. Melting point 62-64 °C.

Difluoro Ester 11: To a flask was charged DAST (92 g, 570 mmol, 2.5 equiv), dichloromethane (470 g), and 2,6-lutidine (6.12 g, 57 mmol, 0.25 equiv) and the solution cooled to 10 °C. A solution of the aldehyde **9** (81.6 g, 228 mmol, 1.0 equiv) in dichloromethane (86 g) was added, rinsing with dichloromethane (2 g). The reaction was mixed at 20 °C for at least 12 h until ^{1}H NMR analysis confirmed consumption of **9**. The reaction mixture was transferred into a 10 °C mixture of heptanes (400 g) and 20% K_2HPO_4 (1.0 kg), rinsing with dichloromethane (1.3 g). The lower (aqueous) layer was separated, and the upper layer was washed with a mixture of 20% brine (1.28 kg) and 20% K_2HPO_4 (0.3 kg). The upper product containing layer was concentrated in vacuo to approximately 200 mL and then diluted with 5% KH_2PO_4 solution (320 g). The biphasic mixture was stirred vigorously, and the reaction monitored by ^{1}H NMR to confirm conversion of byproduct **12** to starting aldehyde **9**. To the reaction was charged 20% K_2HPO_4 (84 g) and 33% sodium bisulfite solution (50 g). The reaction was stirred until the

aldehyde **9** was converted to the bisulfite complex, confirmed by monitoring the upper layer by ^{1}H NMR for consumption of aldehyde **9**. The mixture was diluted with heptanes (500 g) and the layers were separated. The aqueous layer containing the starting aldehyde as the bisulfite complex was treated with 42 g of sodium carbonate. The aldehyde crystallized out of the mixture and was cooled to 0 °C and filtered, washing with water. The typical recovery of **9** was 35%. The upper product containing heptane layer was washed with 20% brine solution (480 g) and then concentrated in vacuo and used in the next step. The heptane solution contained **11** (39.7 g by HPLC assay) for a 46% yield. ^{1}H NMR (400 MHz, $CDCl_3$) δ 5.95 (td, *J* = 55.5, 7.1 Hz, 1H), 4.21 (qd, *J* = 7.1, 1.0 Hz, 2H), 2.12 (dddt, *J* = 10.1, 8.6, 7.1, 4.2 Hz, 1H), 1.95 (dddd, *J* = 8.4, 6.4, 2.1, 0.8 Hz, 1H), 1.50 (s, 19H), 1.27 (t, *J* = 7.1 Hz, 3H). ^{13}C NMR (101 MHz, $CDCl_3$) δ 169.41, 151.38, 114.98 (dd, *J* = 238.8, 232.8 Hz), 83.53, 62.27, 42.33 (d, *J* = 10.3 Hz), 34.66 (dd, *J* = 34.4, 30.4 Hz), 28.33, 22.64 (d, *J* = 7.5 Hz), 14.61. ^{19}F NMR (564 MHz, Chloroform-*d*) δ -110.05 (dd, *J* = 293.6, 55.3 Hz), -114.34 (ddd, *J* = 293.2, 55.8, 8.7 Hz). HRMS calcd $C_{17}H_{27}F_2NNaO_6$ $[M+Na]^+$: 402.1699, Found 402.1711. A sample of **11** crystallized from heptane for characterization and showed a melting point of 73-74 °C. Full characterization of byproduct **12** was not possible due to decomposition upon purification however NMR analysis of the product mixture after aqueous workup provided data that allowed the structural assignment. Byproduct **12** exists as two stereoisomers that exhibit diagnostic signals in the ^{1}H NMR spectrum for the hydrogen atom labeled H_a in Table 1. The major isomer has a 90° dihedral angle between H_a and the adjacent hydrogen resulting in a doublet due to coupling only to fluorine. The minor stereoisomer shows coupling to fluorine as well as the adjacent hydrogen resulting in a doublet of doublets. The ratio between the major and minor stereoisomers of **12** is approximately 2:1 based on the integration of the ^{1}H and ^{19}F NMR signals. The CH_2 of the ethyl group in **12** is

shifted upfield and the hydrogens are diastereotopic. The select diagnostic signals for byproduct **12** are ^{1}H NMR (600 MHz, $CDCl_3$) δ 5.63 (d, *J* = 65.2 Hz, 1H, major), 5.60 (dd, *J* = 64.6, 7.7 Hz, 1H, minor) for H_a stereoisomers, and for the CH_2 of the ester δ 3.92 (dqd, *J* = 9.7, 7.1, 1.2 Hz, 1H), 3.85 (dqd, *J* = 9.8, 7.1, 2.8 Hz, 1H), and for ^{19}F NMR (564 MHz, Chloroform-*d*) δ -76.51 (minor), -87.32 (major), -114.50 (d, *J* = 67.1 Hz, major), -115.07 (d, *J* = 65.0 Hz, minor). The structure of the alkene impurity **13** is based on the following NMR data for a mixture of **11** and **13** showing the presence of a fluorine substituted alkene and two fluorine atoms. The alkene configuration was assigned based on the following signals: ^{1}H NMR (400 MHz, $CDCl_3$) δ 6.51 (ddt, *J* = 83.2, 11.5, 1.3 Hz, 1H), 5.35 (dddd, *J* = 17.1, 11.2, 9.4, 6.7 Hz, 1H), 2.86 (ddddd, *J* = 14.4, 9.7, 6.6, 3.0, 1.6 Hz, 1H), 2.70 (dddd, *J* = 24.0, 14.6, 9.4, 1.0 Hz, 1H). ^{19}F NMR (564 MHz, Chloroform-*d*) δ -122.24 (dd, *J* = 83.4, 17.2 Hz), -125.49 (dd, *J* = 24.6, 9.9 Hz).

Amino Acid 8: The starting material **11** as a solution in heptane (8.05 g, 21.2 mmol) was concentrated in vacuo, chased with EtOH, and then dissolved in EtOH (38.1 g) and THF (43.1 g). The solution was heated to 50 °C and then a 5.5% solution of LiOH (46.2 g, 106 mmol, 5.0 equiv) was added and the mixture stirred at 50 °C until the reaction is complete by HPLC analysis (approximately 10 h). The mixture was cooled to 20 °C and then 49% formic acid (7.01 g, 74.7 mmol, 3.5 equiv) was added and the mixture concentrated in vacuo to approximately 60 mL. To this mixture was added *i*-PrOAc (70 g) and 49% formic acid (5.03, 53.6 mmol, 2.5 equiv) to adjust the pH to ~4.5. The mixture was filtered through a pad of celite (1.3 g), rinsing with *i*-PrOAc (30 g) and the layers separated. The upper product containing layer was washed with water (40 g), and then 20% brine (45 g). The *i*-PrOAc solution was concentrated in vacuo, chased with *i*-PrOAc, and concentrated to a volume of approximately 11 mL and the product crystallized. The slurry was diluted with heptanes (36.5 g) and mixed for 3 hours at 20 °C and

then filtered, rinsing with a mixture of *i*-PrOAc (2.8 g) and heptanes (19.8 g). The solid was dried and the yield of **8** was 85% (4.6 g, 98.2% potency). Rotational isomers were observed, complicating the NMR spectra for compound **8**. ^{1}H NMR (400 MHz, DMSO-d_6) δ 13.00 (s, 1H), 7.80 – 7.21 (m, 1H), 5.92 (tdd, J = 55.9, 15.8, 7.4 Hz, 1H), 2.04 – 1.77 (m, 1H), 1.75 – 1.55 (m, 1H), 1.37 (s, 10H). ^{13}C NMR (101 MHz, DMSO-d_6) δ 172.31, 155.43, 116.34 (dd, J = 237.0, 232.0 Hz), 78.28, 36.78 (d, J = 9.4 Hz), 30.13 (t, J = 31.8 Hz), 28.17, 19.04 (d, J = 8.1 Hz). HRMS calcd $C_{10}H_{15}F_2NNaO_4$ $[M+Na]^+$: 274.0861, Found 274.0859. Melting point 139-141 °C.

Amino Sulfonamide 2: The amino acid **8** (4.88 kg, 4.46 kg potency adjusted, 17.8 mol, 1.0 equiv), 1-methylcyclopropane-1-sulfonamide **7** (3.30 kg, 24.2 mol, 1.26 equiv), and HATU (8.71 kg, 22.9 mol, 1.18 equiv) were charged to a reactor followed by acetonitrile (46.2 kg) and the mixture cooled to 15 °C. Then 2,6-lutidine (2.68 kg, 25.0 mol, 1.29 equiv) was added while maintaining an internal temperature below 25 °C. The solution was cooled to 15 °C and DMAP (9.50 kg, 77.8 mol, 4.0 equiv) was added while maintaining an internal temperature below 25 °C. The resulting slurry was stirred for 16 h at 20 °C and HPLC analysis showed complete consumption of starting material **8**. The reaction was filtered, and the solids were washed with acetonitrile (30 kg). *i*-PrOAc (70 kg) was added to the filtrate and the solution washed with 20 wt% phosphoric acid (3 × 82 kg) and then diluted with *i*-PrOAc (24 kg). The product solution was then washed with 2 wt% phosphoric acid (80 kg) and then with water (4 × 100 kg and 1 × 5 kg), diluting with *i*-PrOAc as needed after each wash (91 kg total). The *i*-PrOAc solution was passed through an inline carbon filter, rinsing with *i*-PrOAc (71 kg). The filtrate was concentrated by vacuum distillation to a volume of 55 L, diluted with *i*-PrOAc (50 kg), and concentrated to a volume of 79 L. The water content of the slurry was <0.02%. The slurry was cooled to 0 °C and anhydrous HCl in *i*-PrOH (16.2 kg at 18.6 wt%, 3.01 kg of HCl, 82.6 mol,

4.26 equiv) was added. The slurry was warmed mixed at 20 ± 10 °C for 40 h and HPLC analysis showed the Boc intermediate was consumed. The slurry was diluted with heptanes (45 kg) and mixed 20 °C for 4 h. The solids were filtered, washed with heptanes (14 kg), and dried under vacuum to afford amino sulfonamide **2** (4.395 kg, 96.55% potency, 15.8 mol) for a yield of 89% over the two steps. Data for **2**: ^{1}H NMR (400 MHz, DMSO-d_6) δ 10.72–8.69 (m, 4H), 5.90 (td, J = 55.5, 6.6 Hz, 1H), 2.37 (tdd, J = 13.9, 8.7, 5.1 Hz, 1H), 2.05–1.97 (m, 1H), 1.76 (ddd, J = 10.1, 6.7, 3.2 Hz, 1H), 1.44 (s, 3H), 1.43–1.38 (m, 1H), 1.38–1.25 (m, 1H), 0.90 (q, J = 2.8 Hz, 2H). ^{13}C NMR (101 MHz, DMSO-d_6) δ 164.68, 114.81 (dd, J = 237.7, 235.1 Hz), 38.69 (d, J = 8.9 Hz), 36.38, 26.95 (dd, J = 34.0, 29.4 Hz), 17.38, 13.67 (d, J = 7.4 Hz), 13.15, 12.39. HRMS calcd $C_9H_{14}F_2N_2NaO_3S$ $[M+Na]^+$: 291.0585, Found 291.0580. Melting point 191-206 °C with decomposition.

Alcohol 22: BF_3 etherate (0.32 g, 2.25 mmol, 0.013 equiv) was added to 140 mL of toluene precooled to 5 °C. To the resulting solution was added a mixture of allyl alcohol (43.5 g, 750 mmol, 4.4 equiv) and cyclopentene oxide (14.5 g, 172 mmol, 1.0 equiv) in toluene (40 mL) over 2 h at 0 to 5 °C. The mixture was warmed to RT over approximately 3 h and mixed overnight. The mixture was cooled to 10 °C and quenched with 50 mL of 10% K_2CO_3 added in one portion. The mixture was stirred for 20 min at 10 to 15 °C and the layers were separated. The toluene layer was washed again with 50 mL of 10% K_2CO_3. The toluene layer was concentrated in vacuo to 26.6 g of oil which was analyzed by HPLC for an assay yield of **22** of 77% (18.9 g). A 25 g aliquot was separated and distilled under vacuum. The main fraction (16.0 g) was collected at 62 to 67 °C and ~3 mm Hg for a 69% adjusted yield. The spectral data were identical to data previously reported in the literature.[33]

Acetate 23: To a reactor was charged **22** (33.6 kg, 236 mol, 1.0 equiv), heptanes (142 kg), and DIPEA (36.3 kg, 281 mol, 1.2 equiv), followed by a rinse of heptanes (6.5 kg). To this solution was added DMAP (270 g, 2.2 mol, 0.0094 equiv) and the solution was then cooled to -5 °C. To this solution was then added acetic anhydride (25.8 kg, 253 mol, 1.07 equiv) over approximately 30 minutes maintaining the temperature below 10 °C. The charge line was rinsed with heptanes (16.2 kg) and the reaction mixed at 0 °C. After mixing for 11 h, a sample was analyzed by HPLC and showed complete conversion of the starting material. The reaction was quenched with 2.5% H_3PO_4 (397 kg) while maintaining the temperature at NMT 10 °C and the mixture was then warmed to RT and the layers were mixed, settled and separated. The aqueous layer was re-extracted with 40 kg of heptanes and this was combined with the first heptane extract. The heptane layer was then successively washed with 68 kg of 20% brine, 81 kg of 5% H_3PO_4, and then 2 × 116 kg of 20% brine. The heptane layer was then concentrated at a vacuum of approximately 220 mm Hg and a jacket temperature of NMT 55 °C. The solution was concentrated in vacuo until near completion and the final volume was 50 L. A final sample was taken for analysis and showed 97.1 area% purity with no starting material detected. The product oil was taken directly into the enzymatic resolution. The typical yield of **23** was ~100%. ^{1}H NMR (400 MHz, $CDCl_3$) δ 5.90 (ddt, *J* = 17.2, 10.4, 5.5 Hz, 1H), 5.27 (dq, *J* = 17.2, 1.7 Hz, 1H), 5.19–5.14 (m, 1H), 5.08–5.03 (m, 1H), 4.04 (qdt, *J* = 12.8, 5.6, 1.5 Hz, 2H), 3.87–3.82 (m, 1H), 2.14–2.05 (m, 1H), 2.04 (s, 3H), 2.00–1.90 (m, 1H), 1.84–1.55 (m, 4H). ^{13}C NMR (101 MHz, $CDCl_3$) δ 170.55, 134.92, 116.79, 83.84, 79.41, 70.28, 30.51, 30.32, 21.70, 21.31. HRMS calcd $C_{10}H_{17}NaO_3$ $[M+Na]^+$: 207.0992, Found 207.1005.

Alcohol 14: To the reactor containing the acetate **23** (theory 43.5 kg, 236 mol) described above was charged a phosphate buffer solution at pH 7 prepared from water (550 kg), K_2HPO_4

(25.0 kg, 144 mol, 0.61 equiv) and KH_2PO_4 (12.0 kg, 88.2 mol, 0.37 equiv). To this mixture was charged Novozym 435 (1.33 kg, 3 wt% relative to **23**) and the mixture stirred at 20 °C. The reaction was deemed complete after 24 h with less than 1.5% of the (*R,R*)-acetate of **23** by chiral HPLC analysis. After mixing for 25 h, 140 kg of solid sodium chloride was added to the reactor followed by 5 kg of celite and the mixture stirred for 1 h. The mixture was filtered through a bed of celite with backup filters. The reactor was rinsed with 180 kg of toluene and the rinse was transferred through the filter setup collecting with the first filtrate. The mixture was transferred to a clean reactor and the reactor and transfer line rinsed with 20 kg of toluene. The mixture was stirred, settled and the layers were separated. The aqueous layer was then re-extracted with 175 kg of toluene, and then 105 kg of toluene. The toluene extracts were then combined and concentrated by vacuum distillation at a pressure of approximately 100 mm Hg and a jacket temperature of NMT 55 °C to a volume of approximately 150 L. The solution was then transferred to a container and the reactor and transfer line rinsed with 10 kg of toluene. The total solution weight was 141.3 kg and assayed for a 47% yield (15.56 kg, < 0.1% of enantiomer) of the (*R,R*)-alcohol **14**. The solution also contained the (*S,S*)-acetate **24** (21.0 kg)

Carbamate 5: To a reactor was charged triphosgene (12.9 kg, 43.5 mol, 0.4 equiv), and a solution of alcohol **14** (141.3 kg, containing 15.56 kg of alcohol **14**, 109 mol, 1.0 equiv) in toluene. To this mixture was added 214 kg of toluene and the solution mixed and then cooled to -10 °C. 2,6-Lutidine (17.7 kg, 166 mol, 1.52 equiv) was added, keeping the temperature below 0 °C. After mixing for 50 min, formation of the chloroformate **25** was complete by GC analysis (alcohol **14** not detected). A quench solution was prepared using 261 kg of 5% NaH_2PO_4 and adjusted to pH 2 with 85% phosphoric acid (6.3 kg, 55 mol) and the solution cooled to 0 °C. The reaction mixture was transferred into the quench solution while maintaining the temperature

below 10 °C, and completing the transfer with a rinse of 40 kg of toluene and then a rinse of 20 kg of water. The layers were mixed at 0 °C and the layers were separated and the toluene layer was washed with 300 kg of cold 20% brine. The toluene solution of the chloroformate **25** was used directly in the next reaction.

To a reactor was charged *tert*-leucine **15** (17.1 kg, 130 mol, 1.2 equiv), water (326 kg) and NaOH (9.6 kg, 240 mol, 2.2 equiv) and the solution mixed and cooled to 0 °C. To this solution mixing at high rpm was added the toluene solution of the chloroformate **25** over 25 minutes, rinsing with 20 kg of toluene, and keeping the temperature below 15 °C. The reaction temperature was held at 5 °C for 2 h, and then warmed to 20 °C. The reaction was complete by GC analysis (< 1% of **25** remaining) after mixing for 11 h, the mixing was stopped and the layers were allowed to settle. The aqueous layer containing the product was separated, the toluene layer was washed with 20 kg of water and the aqueous extracts were combined. To the product solution was added 15 kg of sodium chloride and mixed to dissolve the solids. The solution was then diluted with 63 kg of *i*-PrOAc and 281 kg of heptanes. The pH of the aqueous layer was adjusted to 2.5 using 85% phosphoric acid (21.3 kg), and the layers were mixed, settled and separated. The *i*-PrOAc/heptane layer was then washed with 400 kg of 20% brine. The *i*-PrOAc/heptane layer was filtered through a bed of magnesium sulfate (3 kg) and a bed of celite (9 kg), then rinsed with 25 kg of heptanes. Assay of the filtrate showed that it contained 28.6 kg (95.4 mol) of the free acid of **5**. To this solution was added water (2.1 kg, 117 mol, 1.2 equiv relative to assay of **5**) and dicyclohexylamine (17.3 kg, 95.4 mol, 1.00 equiv relative to assay of **5**). After mixing at RT for 2 h, the product crystallized and a white slurry was obtained. The slurry was filtered and rinsed with 30 kg of heptane. The solid was dried in a vacuum oven at RT to afford carbamate **5**. (46.58 kg, 98.8 area% purity, 90.2% potency as the dicyclohexylamine

salt) for an 80% yield. The isolated solid contained residual heptanes. For NMR characterization a sample was dried at 85 °C to remove the residual solvent. ^{1}H NMR (400 MHz, DMSO-d_6) δ 6.12 (d, J = 8.5 Hz, 1H), 5.85 (ddt, J = 17.2, 10.5, 5.3 Hz, 1H), 5.21 (dq, J = 17.2, 1.8 Hz, 1H), 5.10 (dq, J = 10.5, 1.5 Hz, 1H), 4.77 (dt, J = 6.2, 2.9 Hz, 1H), 4.06 – 3.90 (m, 2H), 3.76 (dt, J = 6.3, 3.3 Hz, 1H), 3.51 (d, J = 8.6 Hz, 1H), 2.93 (tt, J = 10.8, 3.8 Hz, 2H), 2.06 – 1.79 (m, 6H), 1.78 – 1.45 (m, 10H), 1.37 – 1.13 (m, 8H), 1.06 (qt, J = 11.9, 3.2 Hz, 2H), 0.89 (s, 9H). ^{13}C NMR (101 MHz, DMSO) δ 172.99, 155.43, 135.33, 116.05, 83.30, 78.37, 69.21, 63.93, 51.65, 34.09, 30.05, 29.81, 29.26, 27.08, 25.09, 24.18, 21.20. HRMS calcd $C_{15}H_{25}NNaO_5$ $[M+Na]^+$: 322.1625, Found 322.1632. Melting point 88–91 °C.

Alcohol 32: To a reactor was added indium (2.44 kg, 21.3 mol, 0.67 equiv), and the reactor flushed with nitrogen for 5 min. To another reactor was charged THF (56 kg) and water (20 kg) and the mixture was cooled to 15 °C and sparged with nitrogen for 15 min. The sparged solvent mixture was transferred with nitrogen pressure to the reactor containing indium and the mixture stirred and cooled to 15 °C. To the reactor was added the 3-bromo-3,3-difluoroprop-1-ene **30** (5.0 kg, 32 mol. 1.0 equiv) over 25 min maintaining the temperature at NMT 30 °C. After mixing for 2 h at 20 °C the indium had dissolved, and a sample was analyzed by HPLC and assayed for 0.6% of residual bromide starting material **30**. After 2.8 h, the reaction was cooled to 15 °C and then added the ethyl 2-oxoacetate **31**, as a 50% solution in toluene (5.87 kg, 28.7 mol, 0.9 equiv) over 30 min while maintaining the temperature at NMT 30 °C. The reaction was mixed for 1.5 h at 20 °C and the assay yield of **32** was 90.3% yield by HPLC analysis. The reaction was cooled to 15 °C and transferred to another reactor, rinsing with 8 kg of THF, and held for workup. The reaction was conducted three more times at roughly the same scale and the four batches were combined for workup (total of 126 mol of **30** charged). The four reaction

mixtures were combined and then quenched with 96 kg of 15% H_3PO_4 (149 mol, 1.18 equiv) and then added 240 kg of MTBE. The layers were mixed, settled, and separated. The THF/MTBE layer was then washed with 200 kg of water, 200 kg of 5% KH_2PO_4, 200 kg of 5% $NaHCO_3$, and 250 kg of 20% brine. The final THF/MTBE layer was filtered, and the reactor rinsed with 2 × 20 kg of MTBE and the combined filtrate was concentrated in vacuo to 100 L and then chased with 2 × 130 kg of EtOAc back to 100 L volume. The solution was filtered through a pad of celite and rinsed with 124 kg of EtOAc. The filtrate was concentrated in vacuo to 40 L volume, filtered into a pressure canister, rinsing 2 × 4 kg of EtOAc. The solution contained **32** (19.2 kg by HPLC assay, 99.3 area% purity by GC analysis) for an 84.3% yield. ^{1}H NMR (400 MHz, $CDCl_3$) δ 6.00 (ddt, *J* = 17.3, 11.8, 11.1 Hz, 1H), 5.75 (dtd, *J* = 17.3, 2.4, 0.8 Hz, 1H), 5.57 (dt, *J* = 11.0, 0.7 Hz, 1H), 4.42–4.24 (m, 3H), 3.26 (d, *J* = 7.0 Hz, 1H), 1.34 (t, *J* = 7.1 Hz, 3H). ^{13}C NMR (101 MHz, Chloroform-*d*) δ 169.72 (dd, *J* = 3.3, 2.2 Hz), 129.52 (t, *J* = 25.3 Hz), 121.90 (t, *J* = 9.4 Hz), 117.88 (t, *J* = 247.1 Hz), 73.08 (t, *J* = 31.3 Hz), 63.06, 14.22. HRMS calcd $C_7H_{11}F_2NaO_3$ $[M+Na]^+$: 203.0490, Found 203.0494.

Quinoxaline 33: A solution of alcohol **32** (19.25 kg, 1.0 equiv, 107 mol) in EtOAc (59 kg) and DMSO (63 kg) was cooled to 0 °C and then T3P (82 kg, 128 mol, 1.2 equiv as a 50% solution in ethyl acetate) was added to over 1.5 h while maintaining the reaction temperature at 0 to 5 °C. A charge of 5.7 kg of EtOAc was added to rinse the charge line. Mixing was continued at 0 °C for 1 h, then the reaction mixture was warmed to RT over 1 h. Mixing was further continued at RT (typically 12 to 17 h) until less than 5 area% of **32** was detected by GC relative to product **28**. The mixture was cooled to 0 °C and Et_3N (27 kg, 267 mol, 2.5 equiv) was added over 30 min while maintaining the temperature at less than 15 °C. The pH of the reaction mixture was adjusted to 4.5 to 5.5 with acetic acid (4 kg, 70 mol, 0.6 equiv). The mixture was cooled to 0 °C

and then phenylenediamine **29** (11.0 kg, 101 mol, 0.95 equiv) was added as a solution in EtOAc (14 kg) and DMSO (16 kg) over 30 min while maintaining the internal temperature at LT 15 °C. A rinse of EtOAc (5 kg) was used to complete the charge. The mixing was continued at 15 °C until the reaction was complete (less than 5% ketone **28** by GC). The mixture was then cooled to 5 °C and quenched by water addition (180 kg) over 1 h while maintaining the internal temperature at LT 25 °C. The pH was adjusted to 7 with 50% NaOH (5 kg) and acetic acid (1 kg). The reaction mixture was then concentrated by vacuum distillation to remove EtOAc and Et_3N to the target volume of approximately 280 L. Product precipitation was observed at this point. The mixture was then further diluted with water (180 kg) to precipitate remaining product. The product was then filtered, and the cake washed with a solution of water (40 kg) and MeCN (10 kg). The product was dried at 45 °C to less than 0.5% water content by KF. The process was conducted twice on scale (19.2 kg of **32**) and the average yield of **33** was 86%. ^{1}H NMR (400 MHz, DMSO-d_6) δ 12.80 (s, 1H), 7.84 (dd, J = 8.4, 1.4 Hz, 1H), 7.62 (td, J = 7.6, 1.4 Hz, 1H), 7.39–7.28 (m, 2H), 6.54 (dq, J = 17.5, 11.3 Hz, 1H), 5.78 (dt, J = 17.5, 2.6 Hz, 1H), 5.64 (d, J = 11.1 Hz, 1H). ^{13}C NMR (101 MHz, DMSO-d_6) δ 152.28, 150.38 (t, J = 27.2 Hz), 133.05, 132.23, 131.19 (t, J = 26.1 Hz), 130.27, 129.47, 123.79, 121.31 (t, J = 9.2 Hz), 116.25 (t, J = 242 Hz), 115.59. HRMS calcd $C_{11}H_8F_2N_2NaO$ $[M+Na]^+$: 245.0497, Found 245.0496. Melting point 177-179 °C.

Chloro Quinoxaline 27: To a reactor was charged **33** (20.35 kg, 95.9% potency, 87.8 mol, 1.0 equiv), and then DMF, (1.4 kg, 1.9 mol, 0.2 equiv), and then isopropyl acetate (89 kg). The mixture was stirred at RT and then thionyl chloride (15.8 kg, 133 mol, 1.5 equiv) was added over 5 minutes. The reaction mixture was then heated to 60 °C for 16 h and HPLC analysis showed 0.2% of **33**. The reaction was cooled to 0 °C and then quenched with 120 kg of water and the

mixture was diluted with 125 kg of heptanes and warmed to RT. The reaction was then filtered, rinsing with 10 kg of heptanes, and then mixed, settled, and the layers separated. The *i*-PrOAc/heptane layer was then washed with 120 kg of water, twice with 120 kg of 10% K_2HPO_4, and 150 kg of 20% brine. The *i*-PrOAc/heptane layer was then filtered through a pad of magnesium sulfate and rinsed with 2 × 10 kg of heptanes. The solution was concentrated in vacuo to approximately 120 L and chased distilled with 170 kg heptanes maintaining a volume of 120 L. The solution was diluted with 40 kg heptanes and filtered through a pad of silica gel (1.1 kg) covered with a pad of celite (1.6 kg). The filtration was completed by rinsing with 2 × 40 kg of heptanes through the silica gel bed. A sample of the filtrate was analyzed by HPLC and the assay yield of **27** was 96% (20.3 kg). ^{1}H NMR (400 MHz, $CDCl_3$) δ 8.20–8.16 (m, 1H), 8.09–8.05 (m, 1H), 7.93–7.79 (m, 2H), 6.53 (dq, *J* = 17.3, 10.8 Hz, 1H), 5.88 (dt, *J* = 17.3, 2.6 Hz, 1H), 5.70 (d, *J* = 11.0 Hz, 1H). LC-MS ESI calcd $C_{11}H_8ClF_2N_2$ $[M+H]^+$: 241.03, Found 241.05. A sample crystallized from pentane for characterization and the melting point was 40 °C.

Amine 6: Into a reactor was added chloro quinoxaline **27** (22.2 kg, 92.3 mol) as a heptane solution and 31 kg of DMF. The solution was concentrated in vacuo to ~40 L to remove the heptane, and then charged **26** (23.0 kg, 99.5 mol, 1.08 equiv) and 105 kg of DMF. After mixing for 30 min the reaction mixture was cooled to 0 °C. Then a solution of NaOtBu (22.6 kg, 235 mol, 2.55 equiv) in DMF (136 kg) was added over 1.5 h while maintaining the temperature below 10 °C. The reaction was mixed at 0 °C. An additional 1.2 kg (5.2 mol, 0.056 equiv) of solid NaOtBu was added and after 5 h the reaction was complete with 1.9% of **27** remaining. The reaction was quenched by slowly adding 222 kg of water while maintaining the temperature at below 20 °C. The mixture was warmed to RT and then 222 kg of MTBE was added then mixed, settled and the lower layer containing the product was separated. The MTBE layer was extracted

with 89 kg of water and the aqueous extracts were combined. The solution was diluted with 45 kg of water and 490 kg of EtOAc, and the pH adjusted to 3-4 by adding 49 kg of 85% H_3PO_4 (425 mol, 4.6 equiv). The layers were mixed, settled, and separated. The EtOAc layer was washed with water (3 × 222 kg), and 20% brine (225 kg). The EtOAc solution was concentrated in vacuo to 50 L, chased with 170 kg of EtOAc back to 50 L, and dissolved in 110 kg EtOAc and filtered, rinsing with 50 kg EtOAc. The product solution was analyzed by HPLC and the assay yield of **34** was 95% (38.1 kg). The EtOAc solution was concentrated in vacuo to 40 L, and solvent switched to MeOH by chase vacuum distillation (3 × 132 kg) back to 40 L. The product was dissolved in 100 kg of MeOH and the solution of **34** in MeOH (38.1 kg, 87.6 mol) was mixed at 20 °C and a solution of HCl in MeOH solution (180 kg, 13.3 wt%, 657 mol, 7.1 equiv) was added over 1.5 h. The reaction solution was allowed to stir at 20 °C for 24 h and by HPLC showed 95.4 area% for the product. The reaction was concentrated under vacuum to approximately 50 L and a constant volume distillation was performed charging 401 kg of MeOH to maintain the volume at approximately 50 L. To this slurry was added 200 kg of *i*-PrOAc and a constant volume distillation was performed maintaining the volume at approximately 250 L while charging 322 kg of *i*-PrOAc. The slurry was mixed at 15 °C for 4 h and the product was filtered, washed with 60 kg of *i*-PrOAc, dried under vacuum at 40 °C for 29 h to afford **6** (29.4 kg, 96.2% potency) for a 79% yield. ^{1}H NMR (400 MHz, DMSO-d_6) δ 10.50 (s, 2H), 8.10 (dd, J = 8.1, 1.3 Hz, 1H), 7.94–7.84 (m, 2H), 7.75 (ddd, J = 8.4, 6.3, 2.1 Hz, 1H), 6.64 (dq, J = 17.3, 11.3 Hz, 1H), 5.90–5.80 (m, 2H), 5.70 (d, J = 11.0 Hz, 1H), 4.51 (dd, J = 10.9, 7.4 Hz, 1H), 3.92 (dd, J = 13.3, 5.5 Hz, 1H), 3.79 (s, 3H), 3.51 (dt, J = 13.3, 1.5 Hz, 1H), 2.68–2.52 (m, 2H). ^{13}C NMR (101 MHz, DMSO-d_6) δ 167.99, 152.65, 140.34 (t, J = 29.9 Hz), 139.97, 136.75, 132.21, 131.44 (t, J = 26.1 Hz), 129.16, 128.22, 126.76, 121.68 (t, J = 9.2 Hz), 116.45 (t, J = 241.9 Hz),

74.84, 57.78, 53.08, 50.17, 34.05. HRMS calcd $C_{17}H_{18}F_2N_3O_3$ $[M+H]^+$: 350.1311, Found 350.1317. Melting point 188–195 °C.

Diene 4: Dicyclohexylamine salt **5** (35.0 kg, 88.9% potency, 64.7 mol, 1.02 equiv) and HATU (26.5 kg, 69.6 mol, 1.10 equiv) were slurried in acetonitrile (269 kg) at ambient temperature. Formation of a clear solution was observed within 30 min. The solution was then transferred to a vessel containing **6** (25.4 kg, 96.2% potency, 63.3 mol, 1.0 equiv) followed by an acetonitrile rinse (29 kg). The internal temperature was adjusted to 15 °C and diisopropylethylamine (24.5 kg, 190 mol, 3.0 equiv) was then added while maintaining the temperature below 25 °C. The mixing was continued at 20 °C for typically 7–10 h. The mixture was then diluted with toluene (149 kg) and filtered to remove dicyclohexylamine hydrochloride. The cake was washed with toluene (75 kg) and the combined filtrate and wash were further diluted with toluene (25 kg) and water (199 kg). The pH of the mixture was adjusted to ~4 with conc. HCl (7.3 kg) while maintaining NMT 30 °C internal temperature. The layers were separated, and the upper layer was washed with water (199 kg), and aqueous 5% potassium carbonate solution (199 kg). The organic layer was concentrated in vacuo to a volume of 120 L and purified by silica gel plug filtration using 175 kg silica gel pre-wetted with 7 wt% EtOAc in heptanes and eluting with EtOAc/heptanes (25 wt% EtOAc, 735 kg total). The product solution was concentrated in vacuo, solvent switched to toluene and then concentrated to a 40 wt% solution that was used directly in the next step. The process was conducted twice at this scale and the assay yield of **4** was 100% (40 kg, 98.3 PA%). ^{1}H NMR (400 MHz, $CDCl_3$) δ 8.17–8.05 (m, 1H), 7.89–7.82 (m, 1H), 7.81–7.72 (m, 1H), 7.69–7.60 (m, 1H), 6.48–6.22 (m, 1H), 5.97–5.90 (m, 1H), 5.84 (ddt, J = 17.2, 10.7, 5.4 Hz, 1H), 5.76 (dt, J = 17.3, 2.6 Hz, 1H), 5.58 (dd, J = 15.5, 11.0 Hz, 1H), 5.40–5.28 (m, 1H), 5.22 (dq, J = 17.2, 1.7 Hz, 1H), 5.18–5.07 (m, 1H), 4.88–4.78 (m, 1H), 4.70 (t, J = 8.4 Hz,

1H), 4.28 (d, *J* = 9.7 Hz, 1H), 4.23 (d, *J* = 11.6 Hz, 1H), 4.14–4.05 (m, 1H), 4.00 (ddt, *J* = 12.9, 5.4, 1.5 Hz, 1H), 3.91 (ddt, *J* = 12.9, 5.6, 1.5 Hz, 1H), 3.78 (s, 3H), 3.76 (m, 1H), 2.71 (ddt, *J* = 13.9, 7.9, 2.0 Hz, 1H), 2.35 (ddd, *J* = 13.8, 9.1, 4.7 Hz, 1H), 1.92 (ddt, *J* = 24.1, 12.0, 7.3 Hz, 2H), 1.80–1.48 (m, 4H), 1.06 (s, 9H). LC-MS ESI calcd $C_{32}H_{40}F_2N_4NaO_7$ $[M+Na]^+$: 653.28, Found 653.30.

Macrocycle Ester 35: The Zhan 1B catalyst (1.70 kg, 2.32 mol, 7.3 mol%) was dissolved in CH_2Cl_2 (15.1 kg) and toluene (53.5 kg). To a reactor was charged toluene (725 kg, 40 L/kg of **4**) and the solvent sparged with nitrogen and heated to 40 °C. A solution of **4** (20.0 kg, 31.7 mol, 1.0 equiv) in toluene (50 kg) and the solution of the catalyst were added to the reactor containing heated toluene at the same rate over 18 hours. After the addition was complete, small rinses of toluene (15 kg total) were used to complete the addition of **4** and the catalyst. The reaction was allowed to stir at 40 °C for 2 h. Another catalyst charge was prepared (0.25 kg, 0.34 mol, 1.1 mol%) dissolved in CH_2Cl_2 (2.4 kg) and toluene (8.0 kg) and then added to the reaction mixture, rinsing with toluene (5 kg). After mixing for another 15 h at 40 °C the reaction was complete with less than 1% of **4** remaining. The reaction was quenched with imidazole (2.5 kg, 37 mol, 1.2 equiv) and then F1 Filtrol (20 kg) was added and the mixture stirred at 25 °C for 23 h. The mixture was filtered through a silica gel plug (51 kg, 2.6 kg/kg of **4**) wetted with heptanes, and eluted with EtOAc/heptanes (305 kg EtOAc/230 kg heptanes). The product solution was concentrated by vacuum distillation to approximately 100 L, with toluene (23 kg) added during the concentration, and then heptanes (18 kg) was charged. The solution was loaded onto a silica gel plug (133 kg, 6.65 kg/kg of **4**) wetted with heptanes. The product was eluted with a gradient of EtOAc/heptanes as follows: 108 kg EtOAc/461 kg heptanes, 147 kg EtOAc/438 kg heptanes, and 717 kg EtOAc/1639 kg heptanes. The product fractions were combined, concentrated in

vacuo and solvent switched to MeOH. The product solution was analyzed by HPLC and the assay yield of **35** was 71.2% (13.6 kg). A sample was crystallized from a mixture of toluene and heptane for NMR analysis and residual toluene was present in the NMR sample. ^{1}H NMR (400 MHz, $CDCl_3$) δ 8.13 (dd, *J* = 8.3, 1.4 Hz, 1H), 7.85 (dd, *J* = 8.4, 1.4 Hz, 1H), 7.75 (ddd, *J* = 8.3, 7.0, 1.5 Hz, 1H), 7.65 (ddd, *J* = 8.4, 6.9, 1.5 Hz, 1H), 6.43–6.25 (m, 2H), 6.20 (t, *J* = 3.7 Hz, 1H), 5.32 (d, *J* = 10.0 Hz, 1H), 5.00 (dt, *J* = 6.1, 2.2 Hz, 1H), 4.65 (dd, *J* = 10.7, 7.1 Hz, 1H), 4.53 (dd, *J* = 11.8, 2.0 Hz, 1H), 4.46–4.34 (m, 2H), 4.05 (ddd, *J* = 11.6, 7.7, 3.5 Hz, 2H), 3.83–3.77 (m, 1H), 3.75 (s, 3H), 2.67–2.58 (m, 1H), 2.26 (ddd, *J* = 14.3, 10.7, 3.9 Hz, 1H), 2.08–1.89 (m, 2H), 1.80–1.66 (m, 3H), 1.59–1.47 (m, 1H), 1.10 (s, 9H). LC-MS ESI calcd $C_{30}H_{37}F_2N_4O_7$ $[M+H]^+$: 603.26, Found 603.30.

Macrocyclic Acid 3: To a solution of **35** (25.5 kg, 42.3 mol, 1.0 equiv) in MeOH (90 L solution volume containing 60 kg of MeOH) was added 2-MeTHF (102 kg) and the solution cooled below 15 °C. To the solution was then added a solution of NaOH (2.5 kg, 62.5 mol, 1.5 equiv) in water (62.5 kg) and the reaction was mixed at 20 °C. After 6 h the reaction showed <1% of **35** remaining by HPLC analysis. The mixture was cooled to below 15 °C and then water (242 kg) was added, followed by heptanes (81 kg) and 2-MeTHF (102 kg). The pH of the lower layer was adjusted to ~10 with 85% H_3PO_4 (525 g, 4.55 mol, 0.107 equiv). The mixture was stirred for 10 min and then filtered, rinsing with water (20 kg). The filtrate was mixed, settled and the layers separated. The upper layer was washed with water (20 kg) and this was combined with the first aqueous layer. The combined aqueous extracts were diluted with 2-MeTHF (308 kg) and acidified to pH 3 by charging 85% H_3PO_4. (8.4 kg, 73 mol, 1.7 equiv). The layers were mixed, settled and separated. The 2-MeTHF layer was then washed twice with 10% brine (425 kg each). The 2-MeTHF layer was then passed through a bed of magnesium sulfate, rinsing with

2-MeTHF (2 × 20 kg). The filtrate was concentrated in vacuo to approximately 90 L and diluted with 2-MeTHF (43 kg). The solution was diluted with heptanes (48 kg) and mixed until crystallization occurred, and a slurry was formed, and then heptanes (271 kg) was added. The slurry was filtered and rinsed with a mixture of heptanes (27 kg) and 2-MeTHF (9 kg). The wet cake was re-crystallized three times from 2-MeTHF/heptanes using the following procedure. The wet cake was charged back to the crystallization vessel and dissolved in 2-MeTHF (90 kg), and to this solution was added heptanes (43 kg) and the solution mixed until crystallization occurred. The crystallization was completed by charging heptanes (245 kg) and the slurry was then filtered and rinsed with a mixture of heptanes (27 kg) and 2-MeTHF (9 kg). The final solid was dried in a vacuum oven at 30 °C. to afford **3** (23.4 kg, 99.0 area%, 89.3% potency) for an 84% yield. The isolated solid contained residual 2-MeTHF and heptanes that were not removed after high temperature drying and were present in the sample for NMR characterization. ^{1}H NMR (400 MHz, $CDCl_3$) δ 8.13 (dd, *J* = 8.3, 1.4 Hz, 1H), 7.89–7.84 (m, 1H), 7.76 (ddd, *J* = 8.4, 6.9, 1.5 Hz, 1H), 7.66 (ddd, *J* = 8.4, 7.0, 1.4 Hz, 1H), 6.42–6.25 (m, 2H), 6.18 (t, *J* = 3.7 Hz, 1H), 5.43 (d, *J* = 10.0 Hz, 1H), 5.06–4.97 (m, 1H), 4.72 (dd, *J* = 10.5, 7.3 Hz, 1H), 4.58 (dd, *J* = 12.3, 2.0 Hz, 1H), 4.43 (d, *J* = 10.1 Hz, 1H), 4.38 (t, *J* = 6.7 Hz, 1H), 4.06 (dt, *J* = 13.5, 3.4 Hz, 1H), 4.02–3.96 (m, 1H), 3.80 (ddd, *J* = 7.3, 4.4, 1.4 Hz, 1H), 2.69–2.58 (m, 1H), 2.47 (ddd, *J* = 14.4, 10.6, 3.9 Hz, 1H), 2.09–1.88 (m, 2H), 1.79–1.63 (m, 3H), 1.53 (dtd, *J* = 14.1, 7.2, 4.0 Hz, 1H), 1.07 (s, 9H). ^{13}C NMR (101 MHz, DMSO-d_6) δ 172.61, 170.36, 156.52, 152.51 (d, *J* = 3.4 Hz), 140.57 (dd, *J* = 33.5, 24.0 Hz), 140.20, 136.88, 132.70 (t, *J* = 8.2 Hz), 132.04, 129.16, 128.06, 126.67, 126.47 (dd, *J* = 28.3, 23.3 Hz), 115.93 (dd, *J* = 249.0, 236.3 Hz), 81.37, 78.50, 75.50, 65.71, 59.50, 57.58, 53.38, 34.68, 34.40, 31.04, 29.85, 26.29, 22.45. HRMS calcd $C_{29}H_{34}F_2N_4NaO_7$ $[M+Na]^+$: 611.2288, Found 611.2288. Melting point 154-156 °C.

Glecaprevir 1: To a reactor was charged acid **3** (15.4 kg, 91.0% potency, 14.0 kg potency adjusted, 23.8 mol), 2-Hydroxypyridine *N*-oxide (3.4 kg, 31 mol, 1.3 equiv), and EDAC (5.9 kg, 31 mol, 1.3 equiv) followed by MeCN (55 kg) and the mixture stirred at 20 °C for 30 minutes. In another reactor was charged sulfonamide **2** (7.9 kg, 96.9% potency, 7.7 kg potency adjusted, 25 mol, 1.1 equiv), followed by MeCN (55 kg) and the mixture cooled to 15 °C and triethylamine (5.3 kg, 52 mol) was added and the mixture stirred at 15 °C. The activated acid solution from the first reactor was charged to the solution of sulfonamide **2** over 30 min maintaining the temperature below 30 °C. The transfer was completed with a MeCN rinse (11 kg). The reaction was mixed at 20 °C for 13 h and HPLC analysis showed complete consumption of acid **3**. The reaction was quenched with water (14 kg) and then heated to 45 °C. An aliquot of the reaction solution (6.3 kg) was transferred to a mix tank and diluted with a solution of water (4.2 kg) and acetic acid (0.2 kg). The contents of the mix tank stirred until crystallization occurred. A solution of water (63 kg) and acetic acid (3.4 kg) was added to the reaction solution while maintaining the temperature at 45 °C. The slurry of seed crystals in the mix tank was then charged to the reactor, and the transfer was completed rinsing with a solution of MeCN (3 kg) and water (3 kg). The reaction mixture was stirred at 45 °C for 1 h and crystallization occurred. Water (105 kg) was charged to the crystallization slurry over 2 h maintaining the temperature at 45 °C. The slurry was cooled to 20 °C, mixed for 11 h, filtered and the product washed with a solution of MeCN (20 kg) and water (31 kg). The wet cake was blown dry on the filter with nitrogen. The crude product was dissolved in MeOH (306 kg) upon heating to 55 ± 10 °C. Water (165 kg) was added to the solution over 2 h while maintaining the temperature above 50 °C. The slurry was cooled to 20 °C over 3 h, mixed for 1 h and then filtered, rinsing with a solution of MeOH (31 kg) and water (17 kg). The wet cake was blown dry with nitrogen for 2 h and then dried in a vacuum

oven at 65 °C using a nitrogen sweep and humidification to afford **1** (18.75 kg, 94.9% potency, 99.77 area% purity) for an overall yield of 89%. ^{1}H NMR (600 MHz, DMSO-d_6) δ 10.49 (s, 1H), 8.95 (s, 1H), 8.09 (dd, J = 8.4, 1.4 Hz, 1H), 7.90 (dd, J = 8.4, 1.8 Hz, 1H), 7.86 (ddd, J = 8.4, 6.8, 1.5 Hz, 1H), 7.74 (ddd, J = 8.3, 6.8, 1.6 Hz, 1H), 7.33 (d, J = 8.9 Hz, 1H), 6.47 (ddd, J = 19.8, 15.5, 4.2 Hz, 1H), 6.29 (ddt, J = 15.6, 8.8, 4.4 Hz, 1H), 6.04 (t, J = 3.7 Hz, 1H), 5.88 (td, J = 55.7, 7.3 Hz, 1H), 4.90 – 4.83 (m, 1H), 4.47 (d, J = 11.9 Hz, 1H), 4.39 – 4.27 (m, 2H), 4.23 (d, J = 9.2 Hz, 1H), 4.08 – 4.00 (m, 2H), 3.79 – 3.72 (m, 1H), 2.49 – 2.43 (m, 1H), 2.18 (ddd, J = 14.3, 10.9, 3.7 Hz, 1H), 2.06 – 1.96 (m, 1H), 1.95 – 1.84 (m, 2H), 1.81 (t, J = 7.0 Hz, 1H), 1.72 – 1.60 (m, 3H), 1.50 – 1.43 (m, 2H), 1.42 (s, 3H), 1.41 – 1.36 (m, 2H), 1.00 (s, 9H), 0.95 – 0.86 (m, 2H). ^{13}C NMR (151 MHz, DMSO-d_6) δ 172.50, 170.56, 168.89, 156.69, 152.60 (d, J = 3.4 Hz), 140.56 (dd, J = 33.6, 23.8 Hz), 140.19, 136.83, 132.81 (t, J = 8.6 Hz), 132.19, 129.23, 128.17, 126.67, 126.55, 115.92 (dd, J = 247.8, 236.0 Hz), 115.69 (t, J = 233.7 Hz), 81.14, 78.67, 75.64, 65.75, 59.53, 58.68, 53.77, 38.04 (d, J = 9.0 Hz), 36.31, 34.94, 34.34, 31.36 (t, J = 32.4 Hz), 30.99, 29.82, 26.41, 22.49, 19.27 (d, J = 7.7 Hz), 17.54, 13.00, 12.81. HRMS calcd $C_{38}H_{47}F_4N_6O_9S$ $[M+H]^+$: 839.30559, Found 839.30703. The solid becomes amorphous at 150 °C.

AUTHOR INFORMATION

Corresponding Author

* E-mail: russell.cink@abbvie.com

Present Addresses

† The present address for Chen Ding is Arrowhead Pharmaceuticals, 502 South Rosa Road, Madison, WI 53719

Notes

AbbVie and Enanta sponsored and funded the study, contributed to the design, participated in the collection, analysis, and interpretation of data, and in writing, reviewing, and approval of the final publication. All authors are or were employees of AbbVie and may own AbbVie stock.

ACKNOWLEDGMENTS

The authors would like to thank our collaborators at AbbVie Steven J. Wittenberger, Seble Wagaw, Dale Kempf, and Keith McDaniel for helpful discussions, Milad Nazari and Linjie Han for conducting the HRMS analysis, Adrian Anderson, Buyun Chen, Ian Marsden, Marius Naris, Greg Nottingham and Qunying Zhang for analytical support. The authors would like to thank our collaborators at Enanta for sharing the details of the initial medicinal chemistry route, Yat Sun Or, Guoqiang Wang, Yonghua Gai, Jun Ma, Li-Juan Jiang, Jiang Long, and Bin Wang.

Supporting Information. Details on the computational methods, results, and references; NMR spectra for compounds **1-6**, **8**, **9**, **11-13**, **23**, **27**, **32**, **33**, **35**.

REFERENCES

(1) (a) World Health Organization. *Global Hepatitis Report 2017*. (WHO, Geneva, 2017). (b) Martinello, M.; Hajarizadeh, B.; Grebely, J.; Dore, G. J.; Gail V. Matthews, G. V. Management of acute HCV infection in the era of direct-acting antiviral therapy. *Nat. Rev. Gastroenterol. Hepatol*. **2018** *15*, 412. (c) Messina, J. P.; Humphreys, I.; Flaxman, A.; Brown, A.; Cooke, G. S.; Pybus, O. G.; Barnes, E. Global Distribution and Prevalence of Hepatitis C Virus Genotypes. *Hepatology* **2015**, *61*, 77. (d) Hajarizadeh, B.; Grebely, J.; Dore, G. J. Epidemiology and natural history of HCV infection. *Nat. Rev. Gastroenterol. Hepatol*. **2013**, *10*, 553.

(2) EASL Recommendations on Treatment of Hepatitis C 2018. *Journal of Hepatology* **2018**, *69*, 461.

(3) (a) Feld, J. J.; Kowdley, K. V.; Coakley, E.; Sigal, S; Nelson, D. R.; Crawford, D.; Weiland, O.; Aguilar, H.; Xiong, J.; Pilot-Matias, T.; DaSilva-Tillmann, B.; Larsen, L.; Podsadecki, T.; Bernstein, B. Treatment of HCV with ABT-450/r–Ombitasvir and Dasabuvir with Ribavirin. *N. Engl. J. Med.* **2014**, *370*, 159. (b) Deeks, E. D. Ombitasvir/Paritaprevir/Ritonavir Plus Dasabuvir: A Review in Chronic HCV Genotype 1 Infection. *Drugs* **2015**, *75*, 1027. (c) Keating, G. M. Ombitasvir/Paritaprevir/Ritonavir: A Review in Chronic HCV Genotype 4 Infection. *Drugs* **2016**, *76*, 1203.

(4) Zeuzem, S.; Foster, G. R.; Wang, S.; Asatryan, A.; Gane, E.; Feld, J. J.; Asselah, T.; Bourlière, M.; Ruane, P. J.; Wedemeyer, H.; Pol, S.; Flisiak, R.; Poordad, F.; Chuang, W.-L.; Stedman, C. A.; Flamm, S.; Kwo, P.; Dore, G. J.; Sepulveda‐Arzola, G.; Roberts, S. K.; Soto‐Malave, R.; Kaita, K.; Puoti, M.; Vierling, J.; Tam, E.; Vargas, H. E.; Bruck, R.; Fuster, F.; Paik, S.-W.; Felizarta, F.; Kort, J.; Fu, B.; Liu, R.; Ng, T. I.; Pilot‐Matias, T.; Lin, C.-W.; Trinh, R.; Mensa, F. J. Glecaprevir–Pibrentasvir for 8 or 12 Weeks in HCV Genotype 1 or 3 Infection *N. Engl. J. Med.* **2018**, *378*, 354.

(5) Lamb, Y. N. Glecaprevir / Pibrentasvir: First Global Approval *Drugs* **2017**, *77*, 1797.

(6) (a) Grubbs, R. H. Olefin-Metathesis Catalysts for the Preparation of Molecules and Materials (Nobel Lecture). *Angew. Chem. Int. Ed.* **2006**, *45*, 3760 (b) Vougioukalakis, G. C.; Grubbs, R. H. Ruthenium-Based Heterocyclic Carbene-Coordinated Olefin Metathesis Catalysts. *Chem. Rev.* **2010**, *110*, 1746.

(7) Gai, Y.; Or, Y. S.; Wang, Z. Quinoxaline-Containing Compounds as Hepatitis C VIRUS Inhibitors. WO 2009/064975 A1, 2009.

(8) (a) Middleton, W. J. New fluorinating reagents. Dialkylaminosulfur fluorides. *J. Org. Chem.* **1975**, *40*, 574. (b) Lal, G. S.; Pez, G. P.; Pesaresi, R. J.; Prozonic, F. M.; Cheng, H. Bis(2-methoxyethyl)aminosulfur Trifluoride: A New Broad-Spectrum Deoxofluorinating Agent with Enhanced Thermal Stability. *J. Org. Chem.* **1999,** *64,* 7048.

(9) Manuscript in preparation. See also (a) Cink, R. D.; Lukin, K. A.; Leanna, M. R.; Pelc, M. J.; Towne, T. B.; Welch, D. S.; Engstrom, K. E.; Ravn, M. M.; Bishop, R. D.; Zhao, G.; Mei, J.; Kallemeyn, J. M.; Hill, D. R.; Abrahamson, M. J.; Morrill, W. H. Synthetic Route to Anti-Viral Agents. US 9,809,576 B1, 2017 (b) Abrahamson, M. J.; Kielbus, A. B.; Riordan, W. T.; Hill, D. R.; Chemburkar, S. R.; Reddy, R. E.; Towne, T. B.; Mei, J.; Brown, G. J.; Mix, S. Enzymatic Process for the Preparation of (1S,2R)-2-(Difluoromethyl)-1-(propoxycarbonyl)cyclopropanecarboxylic Acid. US 10,316,338 B1 2019 (c) Lukin, K. A.; Mei, J.; Hill, D. R.; Abrahamson, M. J. Difluoroalkylcyclopropyl Amino Acids and Esters, and Syntheses Thereof. US 9,809,534 B1 2017 (d) Abrahamson, M. J.; Chemburkar, S. R.; Kielbus, A. B.; Cink, R. D. Enzymatic Processes for the Preparation (±)-2-(Difluoromethyl)-1-(Alkoxycarbonyl)-Cyclopropanecarboxylic Acid and (±)-2-(Vinyl)-1-(Alkoxycarbonyl)-Cyclopropanecarboxylic Acid. WO 2018/144681 A1, 2018.

(10) Or, Y. S.; Ma, J.; Wang, G.; Long, J.; Wang, B. Macrocyclic Proline Derived HCV Serine Protease Inhibitors. WO 2012/040167 A1, 2012.

(11) Beaulieu, P. L.; Gillard, J.; Bailey, M. D.; Boucher, C.; Duceppe, J.-S.; Simoneau, B.; Wang, X.-J.; Zhang, L.; Grozinger, K.; Houpis, I.; Farina, V.; Heimroth, H.; Krueger, T.;

Schnaubelt, J. Synthesis of (1*R*,2*S*)-1-Amino-2-vinylcyclopropanecarboxylic Acid Vinyl-ACCA) Derivatives: Key Intermediates for the Preparation of Inhibitors of the Hepatitis C Virus NS3 Protease *J. Org. Chem.* **2005**, *70*, 5869.

(12) Formation of a similar cyclic byproduct has been previously reported, see Fukuhara, T.; Hara, S. Polyfluorination Using IF_5. *J. Org. Chem.* **2010**, *75*, 7393.

(13) The identification of impurities **12** and **13** was based on analysis by ^1H NMR. See the experimental section and the Supporting Information for further details.

(14) (a) Umemoto, T.; Singh, R. P.; Xu, Y.; Saito. N. *J. Am. Chem. Soc.* **2010**, *132*, 18199. (b) Beaulieu F.; Beauregard, L. P.; Courchesne, G.; Couturier, M.; LaFlamme, F.; L'Heureux. A. Aminodifluorosulfinium Tetrafluoroborate Salts as Stable and Crystalline Deoxofluorinating Reagents. *Org. Lett.* **2009**, *11*, 5050.

(15) Bòdai, V.; Orocecz, O.; Szakàcs, G.; Novàk, L.; Poppe, L. Kinetic resolution of *trans*-2-acetoxycycloalkan-1-ols by lipase-catalysed enantiomerically selective acylation. *Tetrahedron: Asymmetry* **2003**, *14*, 2605.

(16) Jacobsen, E. N.; Kakiuchi, F.; Konsler, R. G.; Larrow, J. F.; Tokunaga, M. Enantioselective Catalytic Ring Opening of Epoxides with Carboxylic Acids. *Tetrahedron Lett.* **1997**, *38*, 773.

(17) Ready, J. M.; Jacobsen, E. N. Highly Active Oligomeric (salen)Co Catalysts for Asymmetric Epoxide Ring-Opening Reactions. *J. Am. Chem. Soc.* **2001**, *123*, 2687.

(18) Matsunaga, S.; Das, J.; Roels, J.; Vogl, E. M.; Yamamoto, N.; Iida, T.; Yamaguchi, K.; Shibasaki, M. Catalytic Enantioselective *meso*-Epoxide Ring Opening Reaction with Phenolic

Oxygen Nucleophile Promoted by Gallium Heterobimetallic Multifunctional Complexes. *J. Am. Chem. Soc.* **2000**, *122*, 2252.

(19) Zhao, L.; Han, B.; Huang, Z.; Miller, M.; Huang, H.; Malashock, D. S.; Zhu, Z.; Milan, A.; Robertson, D. E.; Weiner, D. P.; Burk, M. J. Epoxide Hydrolase-Catalyzed Enantioselective Synthesis of Chiral 1,2-Diols via Desymmetrization of meso-Epoxides. *J. Am. Chem. Soc.* **2004**, *126*, 11156.

(20) Faber, K.; Riva, S. Enzyme-Catalyzed Irreversible Acyl Transfer. *Synthesis* **1992**, 895.

(21) Kirk, O.; Christensen. M. W. Lipases from *Candida antarctica*: Unique Biocatalysts from a Unique Origin. *Org. Proc. Res. Dev.* **2002**, *6*, 446.

(22) (a) Seyferth, D.; Simon, R. M.; Sepelak, D. J.; Klein, H. A. *gem*-(Difluoroally1)lithium: Preparation by Lithium-Halogen Exchange and Utilization in Organosilicon and Organic Synthesis. *J. Am. Chem. Soc.* **1983**, *105*, 4634. (b) Yang, Z. Y.; Burton, D. J. *Gem*-Difluoroallylation of Aldehydes and Ketones as a Convenient Route to α,α-Difluorohomoallylic Alcohols. *J. Org. Chem.* **1991**, *56*, 1037.

(23) Kirihara, M.; Takuwa, T.; Takizawa, S.; Momose, T. α,α-Difluoroallyl Carbanion: Indium-mediation in Its Facile Coupling with Aldehydes. *Tetrahedron Lett.* **1997**, *38*, 2853.

(24) Chan, T. H.; Yang Y. Indium-Mediated Organometallic Reactions in Aqueous Media: The Nature of the Allylindium Intermediate. *J. Am. Chem. Soc.* **1999**, *121*, 3228.

(25) Meudt, A.; Scherer, S.; Boehm, C. Method for the Production of Aldehydes and Ketones by Oxidizing Primary and Secondary Alcohols with Alkylphosphonic Acid Anhydrides. US 7,262,328 B1, 2007.

(26) The identification of impurities **36**, **37** and **38** was based on LCMS data. Additionally, a sample of impurity **36** was converted to the corresponding daughter impurity in **1** and NMR analysis confirmed the alkene configuration.

(27) The lower conversion observed in entries 4-8 in Table 3 was likely due to the lower catalyst loading, however the impurity profile was not improved relative to entries 1 and 2 and therefore these catalysts were not evaluated further.

(28) Hong, S. H.; Sanders, D. P; Lee, C. W.; Grubbs, R. H. Prevention of Undesirable Isomerization during Olefin Metathesis. *J. Am. Chem. Soc.* **2005**, *127*, 17160.

(29) (a) Itoh, T.; Mitsukura, K.; Ishida, N.; Uneyama, K. Synthesis of Bis- and Oligo-gem-difluorocyclopropanes Using the Olefin Metathesis Reaction. *Org. Lett.* **2000**, *2*, 1431. (b) Chatterjee, A. K.; Morgan, J. P.; Scholl, M.; Grubbs R. H. Synthesis of Functionalized Olefins by Cross and Ring-Closing Metatheses. *J. Am. Chem. Soc.* **2000**, *122*, 3783.

(30) Bochevarov, A. D.; Harder, E.; Hughes, T. F.; Greenwood, J. R.; Braden, D. A.; Philipp, D. M.; Rinaldo, D.; Halls, M. D.; Zhang, J.; Friesner, R. A. Jaguar: A High-Performance Quantum Chemistry Software Program with Strengths in Life and Materials Sciences. *International Journal of Quantum Chemistry* **2013**, *113*, 2110. Schrödinger Release 2018-1: Jaguar, Schrödinger, LLC, New York, NY, 2018.

(31) (a) Caspi, D. D.; Cink, R. D.; Clyne, D.; Diwan, M.; Engstrom, K, M.; Grieme, T.; Mei, J.; Miller, R. W.; Mitchell, C.; Napolitano, J. G.; Nere, N.; Ravn, M. M.; Sheikh, A.; Wagaw, S.; Zhang, H. Process development of ABT-450 - A first generation NS3/4A protease inhibitor for HCV. *Tetrahedron* **2019**, 75, 4271. (b) Wagaw, S.; Ravn, M.; Engstrom, K.; Xu, G.; Wang, Z.;

Sun, Y.; Niu, D; Or, Y. S. Process for making Macrocyclic Oximyl Hepatitis C Protease Inhibitors, WO 2009/073780 Al, 2009.

(32) Chen, S.; Gates, B. D.; Sheikh, A. Y. Crystal Forms. WO 2015/188045 Al, 2015.

(33) Gansäuer, A.; Pierobon, M.; Bluhm, H. Titanocene Catalysed 5-exo Cyclisations of Unsaturated Epoxides– Reagent Control in Radical Chemistry. *Synthesis* **2001**, 2500.